SNARE PROTEIN EVOLUTION AND EXPANSION DRIVES ENDOSOME COMPLEXITY

by

James Hilton Grissom III

A dissertation submitted to the faculty of
The University of North Carolina at Charlotte
in partial fulfillment of the requirements
for the degree of Doctor of Philosophy in
Biology

Charlotte

2023

Approved by:

_____
Dr. Richard Chi

_____
Dr. Andrew Truman

_____
Dr. Adam Reitzel

_____
Dr. Veronica Segarra

_____
Dr. Yuri Nesmelov

ABSTRACT

JAMES HILTON GRISSOM III. SNARE Protein Evolution and Expansion Drives Endosome Complexity. (Under the direction of DR. RICHARD CHI)

The budding yeast *Saccharomyces cerevisiae* is a powerful and well-studied model organism that is responsible for much of our understanding in the fields of endocytosis, the secretory pathway, and membrane trafficking. Traditionally, it was thought that endomembrane systems were highly conserved from yeast to vertebrate cells, with cargo first being internalized at the plasma membrane (PM) before being trafficked to the early endosome via vesicle budding and subsequent fusion. From here, cargo could be recycled back to the PM via recycling endosomes, or remain in the endosome as it matures, eventually being degraded as the late endosome fuses to a lysosome (or the vacuole in yeast). In recent years, there has been confusion in defining the fundamental organelles that comprise the yeast endomembrane system. Some groups have shown that budding yeast has a minimal endomembrane that lacks early and recycling endosomal structures. While others have found specific cargos do sort through recycling endosomes in yeast. With the vast amount of information that has been discovered using the budding yeast endomembrane, the field must now come to understand these pathways in the context of these new paradigms. The aim of this dissertation is to clarify which organelle is accepting post-endocytic vesicles and to determine the fusion machinery that mediates their fusion. Central to membrane fusion is a family of proteins known as SNAREs (Soluble NSF Attachment protein Receptors), which are found on both vesicle and target membrane structures. These SNAREs are localized to distinct membranes and are responsible for specific vesicle fusion events,

making them an excellent lens for studying the endomembrane system. Chapter 1 is a published review that synthesizes what is known about SNARE distribution and interactions in budding yeast. Chapter 2 describes a novel CRISPR-Cas9 strategy we developed to engineer marker-free SNARE mutants in budding yeast. Chapter 3 describes an unpublished study that uses yeast genetic, molecular and evolutionary biology to better understand how SNARE protein evolution and expansion gave rise to complex and modern endosomal systems.

ACKNOWLEDGEMENTS

I would first like to sincerely thank my mentor, Dr. Richard Chi, for all he has done to teach, guide, and push me to give my all; his insight and experience has aided me in becoming the researcher that I am today. He has never hesitated to lend a hand of support or step in to help when someone is struggling, and always strives to see them succeed. His sense of humor is unmatched and his jokes never fail to get a laugh, I will miss being a part of all of the pranks and the friendly banter. I am forever grateful for all he has done and will continue to emulate all he has taught me as I continue my career in research.

I would next like to thank my committee members Dr. Andrew Truman, Dr. Adam Reitzel, Dr. Veronica Segarra, and Dr. Yuri Nesmelov for their input, suggestions, and guidance throughout the course of my dissertation. I would like to thank Dr. Truman for his insight and assistance with utilizing CRISPR/Cas9, his help with using the auxin-inducible degron system to create several yeast strains integral to this dissertation, and for all of the reagents shared between our labs. His enthusiasm and excitement for research and collaboration has been a powerful motivator throughout the entirety of my doctorate. I am thankful to Dr. Reitzel, both for the tremendous amount of assistance he gave in the phylogenetic aspects of my dissertation as well as his genuine interest in the goings on of graduate students in the biology department. Every time we cross paths it is obvious that when he asks how you are doing or how your research is going, he sincerely cares, which has helped instill a very positive and supportive environment in the department. I would next like to thank Dr. Segarra for all the help she gave when I first started in Dr. Chi's lab, for her expertise in writing and yeast biology, and for the encouragement she has

continued to give me over the course of my dissertation. Thank you for always believing in me!

Finally, I would like to thank all of the members of the Chi lab (past and present), and the friends I have made over the course of my doctorate. Whether planning an event, venting together over a beer, cleaning a lab space, or playing Dungeons and Dragons together, your friendship and support means the world to me and I will cherish these relationships always.

DEDICATION

To my wife Nikki,

Whose laughter, love, and light has been my anchor since the beginning.

And to my parents,

who have always encouraged me to go on every adventure, especially this one.

TABLE OF CONTENTS

LIST OF TABLES

LIST OF FIGURES

ABBREVATIONS

Acronyms and Abbreviations

PM - Plasma membrane

TGN- *trans*-Golgi Network

SNARE- Soluble NSF-attachment protein receptor

CME- Clathrin-mediated endocytosis

PCR- Polymerase chain reaction

CRISPR- Clustered regularly interspaced short palindromic repeats

PAM- Protospacer-adjacent motif

gRNA- guide ribonucleic acid

CCV-Clathrin-coated vesicle

PVE- Pre-vacuolar endosome

t-SNARE- target membrane SNARE

v-SNARE- vesicle membrane SNARE

NSF- N-methylmaleimide sensitive fusion protein

α-SNAP- soluble NSF attachment protein α

GFP- Green fluorescent protein

CPY- Carboxypeptidase Y

p1CPY- Carboxypeptidase Y precursor 1

p2CPY- Carboxypeptidase Y precursor 2

ER- Endoplasmic reticulum

PTM- Post-translational modification

ORF- Open reading frame

LB- Luria broth

YPD- yeast extract, peptone, dextrose

bp- base pairs

WT- Wildtype

RME- Receptor-mediated endocytosis

YTK- Yeast Toolkit

BSA- Bovine serum albumin

CSMD- Complete synthetic media with dextrose

ANOVA- Analysis of variance

DIC- Differential interface contrast

FITC- Fluorescein isothiocyanate

HsSNARE- *Homo sapiens* SNARE

COPI- Coat protein complex I

COPII- Coat protein complex II

INTRODUCTION

Clathrin-mediated endocytosis (CME) is one of the most important cellular processes for the uptake of nutrients and other cargos at the cell surface [1, 2]. CME is a specialized form of receptor-mediated endocytosis involving clathrin and other endocytic proteins. During CME more than 60 proteins are recruited to plasma membrane (PM) sites for cargo capture, vesicle formation, and internalization [3, 4]. The budding yeast *Saccharomyces cerevisiae* is a powerful model organism that has led the field in research involving endocytosis and membrane trafficking [5-7]. Many of the pathways and cellular processes in yeast are conserved in human cells; much of what we understand about the endocytic pathway was first discovered in yeast and then later translated to a human model. Because of this, it was assumed that endocytosis and endomembrane organization was highly conserved from yeast to vertebrates, with species specific nuances. In this pathway, cargo first binds to a PM receptor, which causes recruitment of adapter proteins and clathrin to form an inward-budding clathrin-coated pit. Once fully mature, the structure undergoes scission from the PM forming a clathrin-coated vesicle. Next, the vesicle sheds its coat before docking and fusion to the primary endocytic accepting organelle, such as the early endosome. Upon fusion, cargo gradually dissociates from its receptor as the early endosome acidifies and matures- allowing receptor molecules to be recycled back to the PM through the recycling endosome. As the endosome matures, it also exchanges material with the *trans*-Golgi Network (TGN) through bidirectional fusion events, allowing for additional cargo to be recycled through the secretory pathway [8]. Mature endosomes, also commonly referred to as the pre-

vacuolar endosome (PVE) in yeast, fuse to the vacuole (which serves as the lysosome in yeast) for content degradation.

Recent studies suggest that budding yeast has a “minimal endomembrane” system that is fundamentally different from mammalian cells. In this model, the TGN acts as the primary acceptor of endocytic vesicles and is responsible for sorting cargo for degradation and the recycling of receptors back to the PM. However, recently another study was published that found a subset of cargos do traffic through recycling endosomes in yeast, bringing more confusion to the field. The overall aim of this dissertation is to identify the post-endocytic acceptor organelle and determine the fusion machinery that mediates PM vesicles fusion to the TGN in budding yeast. While also aiming to understand how fusion protein evolution and expansion gave rise to modern endosomal systems.

Central to membrane fusion is a family of proteins known as SNAREs (Soluble NSF Attachment Protein Receptors), which are located on both the vesicle and target membrane surfaces. These proteins are known to localize and mediate vesicle fusion with specific membranes because of this are perhaps the most well-suited protein family to define the yeast endomembrane system [9]. While SNAREs have been annotated in many cellular pathways, those mediating the fusion of PM vesicles to the TGN in yeast are not known [10-12]. The first chapter of this dissertation addresses what is known about SNARE fusion machinery and their interactions. This chapter serves to synthesize this information as well as map it to the minimal endomembrane model proposed by Day et al and predicts SNAREs proteins that might mediate the fusion of PM-derived endocytic vesicles to the TGN.

Next, we sought to test our hypothesis by engineering combinational mutants from all 24 SNARE proteins in yeast. However, we encountered technical challenges using traditional methods of genome editing that involve PCR-based gene deletions that incorporate auxotrophic or drug-resistance selectable markers. These methods are limited by the number of available markers that can be used in a single yeast strain, and multiple edits to a single yeast strain significantly decreases efficiency. Since our future experiments required three or more gene edits, we made an effort to improve these methodologies. To accomplish this, we developed a novel strategy to create marker-free edits in yeast. Chapter 2 addresses these limitations and describes a method for marker-free genome editing in budding yeast using CRISPR/Cas9.

In chapter 3, we utilize this CRISPR/Cas9 strategy to create SNARE mutants to help clarify the post-endocytic events after vesicle internalization. We utilized fluorescent α-factor uptake to identify the primary accepting organelle of PM-derived vesicles and determined the subset of SNARE proteins responsible for mediating PM to TGN vesicle fusion in yeast. We also extrapolate these results in the context of eukaryotic endomembrane system evolution. Using an evolutionary phylogenetic analysis of endomembrane-associated SNAREs from yeast and metazoan species, we were able to map a pattern of SNARE homolog expansion across eukaryotic evolution which supported several potential PM to TGN SNARE candidates proposed in Chapter 1. Furthermore, we tested if human SNAREs evolved from ancestral yeast endosomal SNAREs, could alter the yeast endomembrane system. Taken together, our findings support the yeast minimal endomembrane model and highlight the importance of SNARE expansion in the evolution of the eukaryotic endomembrane system.

CHAPTER 1: NEW PERSPECTIVES ON SNARE FUNCTION IN THE YEAST MINIMAL ENDOMEMBRANE SYSTEM

1.1 Abstract

Saccharomyces cerevisiae is one of the best model organisms for the study of endocytic membrane trafficking. While studies in mammalian cells have characterized the temporal and morphological features of the endocytic pathway, studies in budding yeast have led the way in the analysis of the endosomal trafficking machinery components and their functions. Eukaryotic endomembrane systems were thought to be highly conserved from yeast to mammals, with the fusion of plasma membrane-derived vesicles to the early or recycling endosome being a common feature. Upon endosome maturation, cargos are then sorted for reuse or degraded via the endo-lysosomal (endo-vacuolar in yeast) pathway. However, recent studies have shown that budding yeast has a minimal endomembrane system that is fundamentally different from that of mammalian cells, with plasma membrane-derived vesicles fusing directly to a trans-Golgi compartment which acts as an early endosome. Thus, the Golgi, rather than the endosome, acts as the primary acceptor of endocytic vesicles, sorting cargo to pre-vacuolar endosomes for degradation. The field must now integrate these new findings into a broader understanding of the endomembrane system across eukaryotes. This article synthesizes what we know about the machinery mediating endocytic membrane fusion with this new model for yeast endomembrane function.

1.2 Introduction

The budding yeast Saccharomyces cerevisiae has long been regarded as an excellent model organism for studying a wide variety of cellular processes, including endocytosis and the secretory pathway. It was the first eukaryote to have its genome fully sequenced, and many of the proteins found in yeast are conserved in mammalian cells. Additionally, yeast is particularly advantageous for mechanistic studies, as its core machinery is conserved in mammalian cells but with reduced components, making it an efficient and cost-effective model to study essential processes [1–5]. One of the fundamental cellular processes we have come to understand using budding yeast is membrane trafficking in the endomembrane system, which includes endocytosis and associated protein sorting pathways [6–9].

In the case of receptor- or clathrin-mediated endocytosis, cargo first binds to a plasma membrane receptor, which in turn recruits adaptor proteins and clathrin to form an inward-budding clathrin-coated pit. Once fully mature, the structure undergoes scission from the plasma membrane, forming a clathrin-coated vesicle (CCV). Next, the CCV sheds its coat before docking and fusion to the primary endocytic accepting organelle, such as the early/recycling endosome. Upon fusion, cargo is permitted to gradually dissociate from its receptor as the early endosome acidifies and matures—allowing receptor molecules to be recycled back to the plasma membrane via the trans-Golgi network (TGN), which acts as a recycling endosome in yeast [10]. Upon exiting the TGN, the recycled receptors return to the cell surface via the secretory pathway. As the early endosome matures, it also exchanges materials with the TGN through bidirectional fusion events [11]. Mature endosomes, also commonly referred to in yeast as the pre-vacuolar compartments or pre-vacuolar endosomes (PVE), fuse to the vacuole

(which serves as a lysosome in yeast) for content degradation (Figure 1). At each step of the pathway, the docking of vesicles to the proper target endomembrane is guided by tethering factors and Rab proteins, while the fusion of the vesicle to the target membrane is mediated by membrane-bound soluble-NSF-attachment-receptor (SNARE) proteins [12–15]. Likewise, cargo within each organelle can be further sorted into other cellular compartments through pathway specific sorting motifs [16–18]. Multiple target-SNAREs (t-SNAREs) are located on the target membrane, and interact with vesicle-SNAREs (v-SNARE) found on the vesicular membrane. Specific t-SNARE/v-SNARE motifs are thought to bind in cognate bundles to form a hydrophobic coiled-coil structure referred to as a SNAREpin, which brings the vesicle and target membranes into contact [14,15,19]. The close proximity allows fusion between the vesicle and the target membrane.

The v-/t-SNARE interaction hypothesis was first proposed by Rothman et al. [21], and has since been at the center of our understanding of SNARE interaction and cellular distribution [15]. Different SNARE molecules are thought to reside in specific membranes, conferring specificity by mediating fusion steps only at the membranes where they are found [21]. These specific interactions are often referred to as cognate interactions, and any SNARE interactions outside of these specific pairings are referred to as non-cognate or promiscuous. For this reason, SNAREs are typically used as fluorescent markers for cell organelles. While these processes are, for the most part, well-understood, there is still uncertainty with respect to aspects of the endocytic pathway in budding yeast. For example, researchers have yet to identify a set of protein markers that distinctly label the early endosome in yeast, and there has been no evidence as to which set of SNAREs mediate endocytic vesicle fusion to the early endosome, despite the fact

that the entire family of yeast SNARE proteins has been well characterized (Figure 1) [22]. One possible explanation comes from a recent study demonstrating that plasma membrane derived endocytic vesicles dock and fuse to the late Golgi, and not to recycling or early endosomes, as previously thought [23]. In this new model, yeast is proposed to have a minimal endomembrane system, in which the late Golgi functions both as an early endosome and a recycling endosome, serving as a central hub for the endo- and exocytic pathways [23]. This review article aims to reexamine studies that defined SNARE functions in yeast, and to discuss their implications for the emerging model of the yeast minimal endomembrane system and the endocytic pathway.

1.3 Overview of SNARE Function

SNAREs are a family of proteins that contain a conserved 60–70 residue SNARE motif that mediates protein-protein interactions and assembly into an α-helical bundle [15,24]. While the majority of these proteins are typically anchored to their associated membrane at their C-terminus, a small number associate to their target membranes using posttranslational modifications such as prenylation [25]. Their conserved SNARE motif is essential for vesicle fusion, as it allows for the formation of the fusion complex known as a SNAREpin [19]. In some cases, as with Sec9 and Spo20, a single SNARE is able to contribute two SNARE motifs to the complex [26]. When four SNARE motifs interact, the α-helices will entwine with one another to form a “coiled-coil” structure. The center of this coiled-coil structure is comprised of a 15-layer hydrophobic core. The center/zero layer of this core harbors an ionic rather than hydrophobic interaction between conserved glutamine and arginine residues found in the SNARE motif [20]. Furthermore, v-

SNAREs and t-SNAREs are also referred to as R-SNAREs and Q-SNAREs, respectively, due to the conserved arginine or glutamine residues found in the main interaction site of the SNAREpin core [20]. Q-SNAREs are further categorized as Qa-, Qb-, and Qc-SNAREs, depending upon the position of their motifs within the SNAREpin. A SNAREpin is comprised of three t-/Q-SNARE motifs and one v-/R-SNARE motif, each providing a glutamine or an arginine to the main point of interaction in the SNAREpin (the zero ionic layer) [20,27].

SNAREpin formation occurs once the v-SNARE engages and entwines with t-SNAREs, following the vesicle reaching its target membrane. During vesicle formation, the v-SNARE is moved from the donor to the vesicle membrane, along with other membrane proteins that will assist in mediating its fusion. Upon the vesicle reaching the target membrane, tethering factors assist in bringing these structures close enough to allow the v-SNARE and the cognate t-SNAREs to interact. The v- and t-SNAREs are unstructured prior to SNAREpin formation. As the coiled- coil structure forms, it releases energy, as the SNARE motifs are “zippered” from the N-terminus to the C-terminus acting as a catalyst, providing the majority of the force required for membrane fusion [28]. The zippering of the SNAREpin drives the membranes of the vesicle and the target into close enough proximity to enable the opening of a fusion pore, allowing cargo to be transferred from the vesicle to the target organelle (Figure 2). The speed of general SNAREpin fusion was recently calculated to be a tenth of a millisecond [29]. Following membrane fusion, the SNAREpin is disassembled by the ATPase NSF (N-ethylmaleimide sensitive fusion protein) and α-SNAP (soluble NSF attachment protein α) [27]. Moreover, α-SNAP first binds to the SNAREpin to create a 20S particle that is

recognized and bound by the N-terminal binding domain of NSF, causing disassembly of the complex [21,30]. The now-isolated t-SNAREs are then reorganized on the acceptor membrane, while the v-SNAREs are recycled back to the appropriate donor membrane via retrograde pathways, to allow for future fusion steps to occur.

1.4 The Yeast Minimal Endomembrane System

While it has long been assumed that all eukaryotic cells contain multiple endosomal compartments [32], studies in budding yeast have failed to yield any protein markers that distinctly and uniquely label the early/recycling endosomes. Although the fluorescent lipophilic dye FM4-64 is internalized by cells at the plasma membrane and subsequently labels endocytic compartments thought to represent the yeast early endosome, it has also been shown to colocalize with the trans-Golgi marker protein Sec7 within the initial stages of endocytosis [33,34]. This indicates that the TGN may also receive bulk endocytic cargo shortly after internalization, performing at least part of the function associated with the early endosome. Recently, researchers have begun to visualize the yeast endomembrane system using both FM4-64-dependent and -independent methods. Vps8-mCherry and Sec7-mCherry enable visualization of the prevacuolar (PVE) compartment and trans-Golgi, respectively. Traditional recycling/early endosome markers, such as Tlg1, Ypt31 or Chs3 fused to GFP, have been shown to significantly colocalize with Sec7-mCherry [23]. Similarly, both FM4-64 and fluorescently labeled α-factor, a yeast mating pheromone that trafficks to the vacuole for degradation, colocalize with the Golgi marker peaking at 3 min after endocytosis, before moving to the PVE at 10 min, indicating that the Golgi serves as the early endosome in yeast [23]. Improved

fluorescent markers capable of labeling key compartments continue to emerge [35], facilitating more detailed insights into the yeast endomembrane system. Most recently, a study investigating the yeast v-SNARE Snc1 has indicated that one of its interacting proteins, Rcy1, may be responsible for the delivery of endocytic plasma membrane to the TGN [1].

Collectively, these studies describe a new paradigm in which cargo-carrying vesicles, formed by the inward budding of the PM, travel and fuse directly to the Golgi, with receptors recycling back to the PM via Golgi-derived vesicles (Figure 1). Next, cargo targeted for degradation is transferred to the PVE, which acts as a late endosome, retaining cargo for degradation by the vacuole. This model addresses many of the inconsistencies from earlier models, particularly the inability of researchers to discern protein markers that uniquely label the early and recycling endosomes. This new perspective offers the simplest explanation for this issue: That early and recycling endosomes do not exist as distinct structures in Saccharomyces cerevisiae. In the following sections, we aim to review SNARE protein function during endocytosis, in light of the minimal endomembrane system model. SNARE proteins are known to localize and mediate vesicle fusion events with specific membranes, making them ideally suited for studies to define the yeast endomembrane system [21].

i. Candidate PM to TGN SNAREs

In this section, we discuss the candidate SNAREs that could mediate transport from the PM in the yeast minimal endomembrane system. While all yeast SNAREs have been annotated (Figure 1), interestingly, none have been identified as mediating the

fusion of plasma membrane-derived vesicles to the early endosome [14,15,19,22]. However, previous studies have identified several candidates for this role, such as t-SNAREs Tlg1 and Tlg2, which colocalize with TGN markers [33,36]. Tlg1 has been shown to have a role in endosome-TGN vesicle fusion [23]. Additionally, cells ablated for Tlg1 secrete carboxypeptidase precursor 1 (p1CPY). p1CPY is first synthesized in the ER then trafficked to the cis- Golgi, where it is post-translationally modified into p2CPY and ultimately matured via proteolytic cleavage by Pep4 in the vacuole [37]. The accumulation or secretion of p1CPY typically indicates a defect in Golgi trafficking [37]. Interestingly, Tlg1 has also been shown to form a SNAREpin complex with Tlg2 and Vti1 [37]. Vti1 localizes to Golgi membranes, while Tlg2 localizes to the endosome, as well as to the Golgi [38, 39]. These findings suggest that Tlg1 likely has more of a Golgi function than an endosome function. Using the fluorescent dye FM4-64, t-SNARE Tlg2 has also been shown to localize to endocytic intermediates [38]. Upon inhibition of Sec18, a protein responsible for disassembling SNARE complexes, Tlg2 forms a SNARE complex with v-SNARES Snc1/2, confirming its presence on both early endocytic structures as well as the TGN [38].

While v-SNAREs are typically recycled between target membranes and t-SNAREs typically remain only on their resident membranes, Tlg1, Tlg2, and Vti1 are unusual t-SNAREs, because they localize to multiple compartments in yeast (Figure 1). Fluorescently tagged v-SNARE Snc1 localizes to both the plasma membrane and the TGN, supporting its role in endosome-TGN vesicle fusion [33]. Interestingly, the deletion of Tlg1 or Tlg2 prevents or abrogates the plasma membrane localization of Snc1 [33]. These data indicate that Snc1 is recycled back to the plasma membrane through TGN-

derived secretory vesicles. This conflicts with the traditional model in which the early endosome mediates the recycling of cargoes such as Snc1 back to the PM independently of the TGN. One explanation for this finding might be that Snc1 acts as a v-SNARE for plasma membrane-endosome vesicle fusion, undergoing a trafficking cycle that involves internalization from the plasma membrane, then transport to the early endosome and later to the TGN, before being recycled back to the plasma membrane. Given the emerging model that the TGN acts as the early endosome in yeast, an alternative explanation might be that Snc1 acts as a v-SNARE for plasma membrane-TGN vesicle fusion, undergoing a trafficking cycle that involves export from the plasma membrane, then transport to the TGN, followed by recycling back to the plasma membrane.

ii. TGN and PVE SNAREs

Following the internalization of cargos, those destined for degradation continue to the pre-vacuolar endosome via TGN-derived vesicles. The SNARE complex mediating this fusion step is thought to consist of the t-SNAREs Pep12, Vti1, and Syn8, located on the PVE surface, and the v-SNARE Ykt6, found on TGN-derived vesicles. Fractionation studies have indicated that Pep12 and other cognate SNAREs coincide with late endosome markers [40]. Pep12 deletion has also been shown to inhibit the transfer of vacuolar hydrolases from the Golgi to the vacuole, but does not disrupt secretory protein transport [40]. This indicates that Pep12 plays a critical role in the fusion of TGN-derived vesicles to the late endosome/pre-vacuolar compartment. The second t-SNARE in this complex, Vti1, also localizes to pre-vacuolar membranes as well as to the Golgi [39], and subcellular sedimentation studies have revealed that Vti1 co-fractionates with Pep12.

Vti1 directly interacts with Pep12, as well as with the intra-Golgi t-SNARE Sed5 [39]. Pep12 and Vti1 contribute to the formation of a functional SNAREpin with the t-SNARE Syn8. First discovered through BLAST searching, Syn8 was later revealed to be a homolog of the mammalian SNARE protein syntaxin 8 [41]. Researchers have since localized Syn8 to the late endosomes, and have found that Syn8 directly interacts with Pep12, Vti1, Snc1, and Snc2, as well as the v-SNARE Ykt6 [41].

iii. PVE to Vacuole SNAREs

After reaching the late or PVE, the targeting of cargos to the vacuole is thought to be mediated by the v-SNARE Nyv1 and its cognate interactions with the t-SNAREs Vam3, Vti1, and Vam7. Nyv1 was initially found to colocalize with the vacuolar membrane protein Vma1, and additional subcellular fractionation confirmed that Vam3 is enriched on vacuolar membranes [42]. Additional vacuolar fusion experiments demonstrated that both Vam3 and Nyv1 are required for successful fusion [43]. Cells lacking Vam3 accumulate precursor CPY, indicating a role for Vam3 in mediating vesicle fusion to the vacuole [42,44]. Overexpression of either Vam7 in vam3Δ cells or Vam3 in vam7Δ cells resulted in phenotypic rescue of CPY sorting, indicating genetic interaction between the two t-SNAREs [45]. Additional co-immunoprecipitation experiments confirmed their physical interaction [45]. Finally, the addition of anti-Vam7 or anti-Vam3 antibodies directly inhibited vacuole fusion, indicating not only that they function at a similar step, but also that they mediate vesicular fusion to the vacuole [46,47].

iv. Intra-Golgi SNAREs

The final group of SNAREs relevant to the yeast minimal endomembrane system is responsible for mediating intra-Golgi vesicle fusion events. This group consists of the t-SNAREs Gos1, Sed5, and Sft1, as well as the v-SNARE Ykt6. The t-SNARE Sed5 localizes to the Golgi, and Sed5 knockout results in ER to Golgi trafficking defects [48]. Moreover, sed5 mutants also accumulate invertase, indicating that it is responsible for intra-Golgi trafficking [49]. Gos1 was first discovered through its physical interaction with Sed5. Cells ablated for Gos1 accumulate secretory protein precursors, indicating a role in intra-Golgi transport [50]. Sequence analysis has identified Gos1 as a homolog of the human t-SNARE Gos-28, and immunofluorescence experiments in HeLa cells have confirmed colocalization of the yeast and human proteins [50]. Multiple studies have reported direct interactions between Sed5 and Sft1 [25,49]. Sft1 was first discovered through its ability to suppress sed5 temperature sensitive mutants, and sft1 mutants also showed aggregation of invertase and CPY precursors, indicating an intra-Golgi trafficking defect [49]. Finally, the v-SNARE Ykt6 was shown to directly interact with Gos1, Sed5, and Sft1 [25]. Similar to sed5 and sft1 mutants, ykt6 mutant cells are enriched for CPY precursors at non-permissive temperatures, indicating a role for Ykt6 in intra-Golgi vesicle trafficking [25].

1.5 Discussion

The recently proposed yeast minimal endomembrane system has provided a new outlook on eukaryotic endocytic processes. More importantly, this model has clarified many of the field's past irreconcilable details, such as the lack of a universally accepted

protein marker for early/recycling endosomes and lack of clarity of the initial steps of fusion during endocytosis. While many of field's past interpretations were primarily based on mammalian endo-lysosomal systems, the field must now continue to examine how this new perspective fits into all that is known about endocytic processes. In this new perspective, the yeast endomembrane system is thought to be more similar to plants with the TGN, acting as the primary acceptor membrane during endocytosis. Moreover, it is likely that, while earlier ancestral endomembrane systems were even more simplified, animals evolved a highly complex system to accommodate the influx of cellular cargos and evolved multiple pathways for material exchange [51]. This view is supported by the fact that many human and yeast SNAREs can participate in multiple fusion steps [52–54]. However, the exact mechanism through which SNARE proteins can participate in multiple fusion steps or pathways is not known. Below, we describe three potential mechanisms that could explain this SNARE multiplicity of function.

First, many SNAREs are promiscuous binders, and are able to associate in non-cognate combinations [55]. Interestingly, both cognate and non-cognate SNARE complexes are fully functional, and are efficient in lipid fusion experiments [55]. Interestingly, ER SNAREs have been shown to be relatively selective, while endosomal and vacuolar SNAREs are thought to be more promiscuous [56] (Figure 1). For example, the t-SNARE Vti1 is able to form functional SNAREpins for at least three separate fusion steps in the endocytic pathway, and has been localized to multiple subcellular structures in yeast and human cells [37,39,55–60]. Golgi t-SNARE Sed5 has been shown to form non-cognate SNAREpins with t-SNAREs Vti1, Tlg1, and v-SNARE Snc2, and therefore may mediate initial plasma-membraned derived vesicles for fusion [56]. Sed5 has also

been shown to form a non-cognate SNAREpin with the vacuolar SNAREs Vam7, Vti1, and Nyv1 [56]. Gos1, another intra-Golgi t-SNARE, has been shown to form a complete SNAREpin with vacuolar SNAREs, and pairwise interactions with Vti1, as well as the endosomal t-SNARE Pep12 [55,56]. The final intra-Golgi t-SNARE, Sft1, shows similar promiscuous interactions with Vti1 and Pep12 [55]. The v-SNARE Ykt6, responsible for intra-Golgi and TGN-PVE trafficking, can interact with the TGN t-SNARE Tlg1 [56]. Endosomal SNAREs show a similar degree of promiscuity. In addition to interactions with intra-Golgi SNAREs, the endosomal t-SNARE Pep12 interacts with vacuolar SNAREs Vam7 and Nyv1, as well as the plasma membrane v-SNARE Snc2 [55,56]. Additionally, Pep12 has been shown to form a non-cognate SNAREpin with Vti1, Tlg1, and Snc2 [56]. Syn8, another endosomal t-SNARE, only shows promiscuous interactions with the plasma membrane v-SNAREs Snc1/2 [41]. Finally, the vacuolar t-SNAREs Vam3, Vti1, and Vam7 have also been shown to form non-cognate interactions with v-SNARE Snc2 [56]. While, in many cases, non-cognate binding may simply be due to similar cognate pair sequences and structures, the precise mechanisms are not known. We believe the high degree of SNARE promiscuity at the TGN strongly supports the minimal endomembrane model. That is, if the TGN sorts both endocytic and secretory cargo, we would expect to see overlap between SNAREs residing on those structures. In contrast, the ER to Golgi and TGN to PM secretory pathways are more clearly defined and exhibit less SNARE promiscuity [26,61-67] (Figure 1).

Second, regulatory SNARE-interacting proteins such as the Rab family could also be regulating vesicular and target membranes. The Rab family of GTPases are critical for SNARE complex formation, play essential roles in docking vesicles to their target

membrane. They are also found in multiple pathways in the cell [68–71]. Therefore, they are excellent candidates to coordinate SNARE function in multiple fusion events. However, Rab proteins have been found to be nonselective with their respective SNAREs interactions [72], and recent reports indicate that Rabs proteins appear to be compartment-specific rather than transport-step-specific [73]. If this is the case, the Rab proteins could be better targets for organelle markers than SNAREs. Interestingly, there are only eleven Rab proteins in budding yeast, while in metazoans, there are at least sixty [68,69]. Therefore, it is also interesting to speculate about the evolutionary context for the high amounts of Rab gene duplication in mammalian cells, and their possible requirement in regulating endomembrane trafficking.

Third, regulatory post-translational modifications (PTMs) on SNAREs could facilitate complex formation between specific molecules. In fact, in vitro, many of the human SNARE proteins have been shown to contain PTMs [74–76]. These PTMs could in turn regulate SNARE complex formation. For example, the phosphorylation of SNAP-25, a human t-SNARE found on the plasma membrane, directly diminished its ability to interact with syntaxin to form a competent SNAREpin [77]. In yeast, the phosphorylation of the t-SNAREs Sso1 and Sec9 directly affects the binding ability of SNARE inhibitory factors that prevent the formation of SNAREpin complexes [78]. Therefore, it is highly likely that other yeast SNAREs also harbor PTMs that regulate function, however, more research on this topic is needed.

1.6 Acknowledgements

The authors would like to thank colleagues Jeff Coleman, Mandi Ma and members of the Chi lab for their helpful input and critical reading of the manuscript. Figure 2 was created with BioRender.com.

1.7 Figures

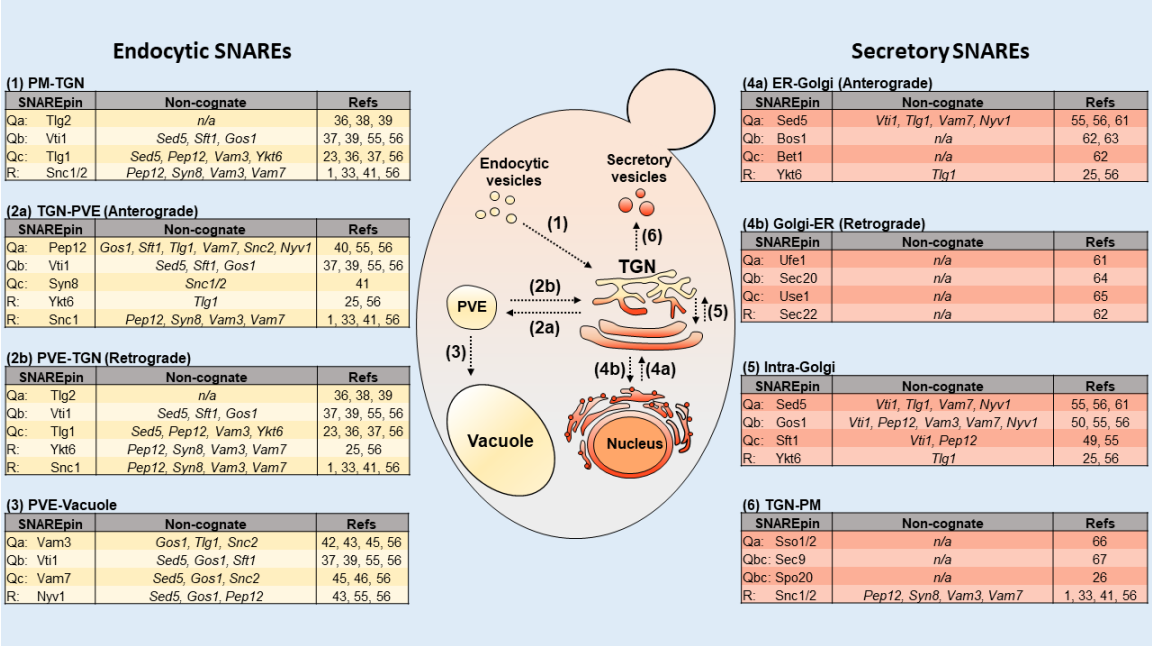

Figure 1. SNARE proteins in the yeast minimal endomembrane system. Center, a cartoon model depicting the yeast minimal endomembrane system. (1) In the endocytic pathway, vesicles fuse with the TGN, within 3 min post-internalization. (2) Cargo destined for degradation is trafficked to the PVE via associated sorting signals within 10 min post-internalization [16]. (2a-b) Cargo is bi-directionally trafficked between the PVE and TGN. (3) PVE cargo fuses to the vacuole for degradation within 30 min post-internalization. (4a-b) Proteins that are synthesized in the rough endoplasmic reticulum (RER) are trafficked to the Golgi. Newly synthesized proteins proceed to the TGN or are returned to the endoplasmic reticulum (ER). (5) Secretory proteins are packaged into vesicles and bud off the TGN. (6) Secretory vesicles fuse to the PM to release cargo. Moreover, v- and t-SNAREs are referred to as R-SNAREs and Q-SNAREs, respectively, due to the conserved arginine or glutamine residues found in the main interaction site of the SNAREpin core [20]. Q-SNAREs are further categorized as Qa-, Qb-, Qc- or Qbc-SNAREs, depending on the position of their SNARE motifs within the SNAREpin. Yellow indicates endocytic pathway and orange indicates the secretory pathway. Left and right tables indicate SNAREs that mediate specific fusion steps. Cognate and non-cognate interactions are also shown.

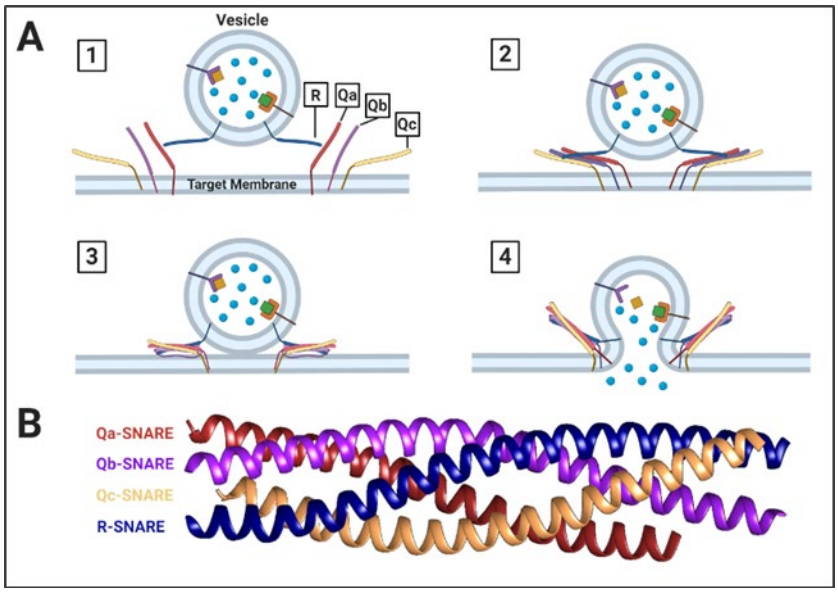

Figure 2. Overview of SNARE Function. (A) (1) Cargo-carrying vesicle with R-SNARE reaches the target membrane, which contains associated Q-SNAREs (not pictured: Rab proteins and other associated tethering factors). (2) The vesicle R-SNARE interacts with 3 target membrane Q-SNAREs to initiate SNAREpin complex formation. (3) The SNAREpin forms a “coiled-coil” quad complex, zippering the vesicle and target membrane bilayers into contact. (4) Membrane fusion occurs, releasing soluble cargo into the lumen of the target membrane. (B) Crystal structure of a Saccharomyces cerevisiae SNAREpin complex [31].

1.8 References

1. Ma, M.; Burd, C.G. Retrograde trafficking and quality control of yeast synaptobrevin, Snc1, are conferred by its transmembrane domain. Mol Biol Cell 2019, 30, 1729-1742, doi:10.1091/mbc.E19-02-0117.
2. D Botstein, G.F. Yeast: an experimental organism for modern biology. Science 1988, 240, 1439-1443.
3. Stacia R. Engel, F.S.D., Dianna G. Fisk, Gail Binkley, Rama Balakrishnan, Maria C. Costanzo, Selina S. Dwight, Benjamin C. Hitz, Kalpana Karra, Robert S. Nash, Shuai Weng, Edith D. Wong, Paul Lloyd, Marek S. Skrzypek, Stuart R. Miyasato, Matt Simison, and J. Michael Cherry. The Reference Genome Sequence of Saccharomyces cerevisiae: Then and Now. Genes Genome Genetics 2014, 4, 389-398.
4. Shahin Mohammadi, B.S., Shankar Subramaniam, Ananth Grama. Scope and limitations of yeast as a model organism for studying human tissue-specific pathways. BMC Sys Biol 2015, 9.
5. Juan S. Bonifacino, B.S.G. The Mechanisms of Vesicle Budding and Fusion. Cell 2004, 116, 153–166.
6. Lu, R.; Drubin, D.G.; Sun, Y. Clathrin-mediated endocytosis in budding yeast at a glance. J Cell Sci 2016, 129, 1531-1536, doi:10.1242/jcs.182303.
7. Boettner, D.R.; Chi, R.J.; Lemmon, S.K. Lessons from yeast for clathrin-mediated endocytosis. Nat Cell Biol 2011, 14, 2-10, doi:10.1038/ncb2403.
8. Chi, R.J.; Harrison, M.S.; Burd, C.G. Biogenesis of endosome-derived transport carriers. Cell Mol Life Sci 2015, 72, 3441-3455, doi:10.1007/s00018-015-1935-x.
9. Ma, M.; Burd, C.G. Retrograde trafficking and plasma membrane recycling pathways of the budding yeast Saccharomyces cerevisiae. Traffic 2020, 21, 45-59, doi:10.1111/tra.12693.
10. Marizela Delic, M.V., Alexandra B. Graf, Martin Pfeffer, Diethard Mattanovich, Brigitte Gasser. The secretory pathway: exploring yeast diversity. FEMS Microbiology Reviews 2013, 37, 872–914.
11. Maria Antonietta De Matteis, A.L. Exiting the Golgi complex. Nature Reviews Molecular Cell Biology 2008, 9, 273-284.
12. Matthijs Verhage, J.B.S. Vesicle Docking in Regulated Exocytosis. Traffic 2008, 9, 1414-1424.
13. Bianka L. Grosshans, D.O., Peter Novick. Rabs and their effectors: Achieving specificity in membrane traffic. PNAS 2006, 103, 11821–11827.
14. Hong, W. SNAREs and traffic. Biochimica et Biophysica Acta 2005, 1744, 120-144.
15. Wang, T.; Li, L.; Hong, W. SNARE proteins in membrane trafficking. Traffic 2017, 18, 767-775, doi:10.1111/tra.12524.
16. Gu, F.; Crump, C.M.; Thomas, G. Trans-Golgi network sorting. Cell Mol Life Sci 2001, 58, 1067-1084, doi:10.1007/PL00000922.
17. Lemmon, S.K.; Traub, L.M. Sorting in the endosomal system in yeast and animal cells. Curr Opin Cell Biol 2000, 12, 457-466, doi:10.1016/s0955-0674(00)00117-4.

18. Feyder, S.; De Craene, J.O.; Bar, S.; Bertazzi, D.L.; Friant, S. Membrane trafficking in the yeast Saccharomyces cerevisiae model. Int J Mol Sci 2015, 16, 1509-1525, doi:10.3390/ijms16011509.
19. Thomas Weber, B.V.Z., James A. McNew, Benedikt Westermann, Michael Gmachl, Fransesco Parlati, Thomas H. Sollner, James E. Rothman. SNAREpins: Minimal Machinery for Membrane Fusion. Cell 1998, 92, 759-772.
20. Suzie J. Scales, B.Y.Y., Richard H. Scheller. The ionic layer is required for efficient dissociation of the SNARE complex by a-SNAP and NSF. PNAS 2001, 98, 14262-14267.
21. Thomas Sollner, M.K.B., Sidney W. Whiteheart, Richard H. Scheller, James E. Rothman. A Protein Assembly-Disassembly Pathway In Vitro That May Correspond to Sequential Steps of Synaptic Vesicle Docking, Activation, and Fusion. Cell 1993, 75, 409-418.
22. Burri, L.; Lithgow, T. A Complete Set of SNAREs in Yeast. Traffic 2004, 5, 45-52, doi:10.1046/j.1600-0854.2003.00151.x.
23. Day, K.J.; Casler, J.C.; Glick, B.S. Budding Yeast Has a Minimal Endomembrane System. Dev Cell 2018, 44, 56-72 e54, doi:10.1016/j.devcel.2017.12.014.
24. Fabienne Paumet, V.R., James E. Rothman. The specificity of SNARE-dependent fusion is encoded in the SNARE motif. PNAS 2004, 101, 3376-3380.
25. James A. McNew, M.S., Nina M. Lampen, Sachiko Machida, R. Ruby Ye, Lynne Lacomis, Paul Tempst, James E. Rothman, Thomas H. Sollner. Ytk6, a prenylated SNARE essential for ER-golgi transport. Journal of Biological Chemistry 1997, 272, 17776-17783.
26. Aaron M. Neiman, L.K., Patrick J. Brennwald. Identification of domains required for developmentally regulated SNARE function in Saccharomyces cerevisiae. Genetics 155, 1643-1655.
27. Yoon, T.Y.; Munson, M. SNARE complex assembly and disassembly. Curr Biol 2018, 28, R397-R401, doi:10.1016/j.cub.2018.01.005.
28. Kienle, N.; Kloepper, T.H.; Fasshauer, D. Phylogeny of the SNARE vesicle fusion machinery yields insights into the conservation of the secretory pathway in fungi. BMC Evol Biol 2009, 9, 19, doi:10.1186/1471-2148-9-19.
29. Manca, F.; Pincet, F.; Truskinovsky, L.; Rothman, J.E.; Foret, L.; Caruel, M. SNARE machinery is optimized for ultrafast fusion. Proc Natl Acad Sci U S A 2019, 116, 2435-2442, doi:10.1073/pnas.1820394116.
30. Tobias M. Hohl, F.P., Chritian Wimmer, James E. Rothman, Thomas H. Sollner, Harald Engelhardt. Arrangement of subunits in 20s particles consiting og NSF, SNAPs, and SNARE complexes. Molecular Cell 1998, 2, 539-548.
31. Strop, P.; Kaiser, S.E.; Vrljic, M.; Brunger, A.T. The structure of the yeast plasma membrane SNARE complex reveals destabilizing water-filled cavities. J Biol Chem 2008, 283, 1113-1119, doi:10.1074/jbc.M707912200.
32. Cristina Prescianotto-Baschong, H.R. Morphology of the Yeast Endocytic Pathway. Molecular biology of the Cell 1998, 9, 173-189.
33. Michael J. Lewis, B.J.N., Cristina Precianotto-Baschong, Howard Riezman, Hugh R. B. Pelham. Specific Retrieval of the Exocytic SNARE Snc1p from Early Yeast Endosomes. Molecular Biology of the Cell 2000, 11, 23-38.

34. Thomas A. Vida, S.D.E. A New Vital Stain for Visualizing Vacuolar Membrane Dynamics and Endocytosis in Yeast. The Journal of Cell Biology 1995, 128, 779-792.
35. Zhu, J.; Zhang, Z.T.; Tang, S.W.; Zhao, B.S.; Li, H.; Song, J.Z.; Li, D.; Xie, Z. A Validated Set of Fluorescent-Protein-Based Markers for Major Organelles in Yeast (Saccharomyces cerevisiae). MBio 2019, 10, doi:10.1128/mBio.01691-19.
36. Joost C.M. Holthius, B.J.N., Sadhana Dhruvakumar, Hugh R.B. Pelham. Two syntaxin homologues in the TGN/endosomal system of yeast. EMBO Journal 1998, 17, 113-126.
37. John G. S. Coe, A.C.B.L., Jing Xu, Wanjin Hong. A Role for Tlg1p in the Transport of Proteins within the Golgi Apparatus of Saccharomyces cerevisiae. Molecular Biology of the Cell 1999, 10, 2407–2423.
38. Hagai Abeliovich, E.G., Peter Novick, Susan Ferro-Novick. Tlg2p, a Yeast Syntaxin Homolog That Resides on the Golgi and Endocytic Structures. THE JOURNAL OF BIOLOGICAL CHEMISTRY 1998, 273, 11719–11727.
39. Gabriele Fischer von Mollard, S.F.N., Tom H. Stevens. The Yeast v-SNARE Vti1p Mediates Two Vesicle Transport Pathways through Interactions with the t-SNAREs Sed5p and Pep12p. The Journal of Cell Biology 1997, 137, 1511–1524.
40. Kathleen A. Becherer, S.E.R., Scott D. Emr, Elizabeth W. Jones. Novel syntaxin homologue, pep12, required for sorting of lumenal hydrolases to lysosome-like vacuole in yeast. Molecular Biology of the Cell 1996, 7, 579-594.
41. Michael J. Lewis, H.R.B.P. A new yeast endosomal SNARE related to mammalian syntaxin 8. Traffic 2002, 3, 922-929.
42. Amit Srivastava, E.W.J. Pth1/Vam3p Is the Syntaxin Homolog at the Vacuolar Membrane of Saccharomyces cerevisae Required for the Delivery of Vacuolar Hydrolases. Genetics 1998, 148, 85-98.
43. Nichols, B.J., Ungermann, Christian, Pelham, Hugh RB, Wickner, William T, Haas, Albert. Homotypic vacuolar fusion mediated by t- and v-SNAREs. Nature 1997, 387, 199-202.
44. Tom Stevens, B.E.a.R.S. Early Stages in the Yeast Secretory Pathway Are Required for Transport of Carboxypeptidase Y to the Vacuole. Cell 1982, 30, 439-448.
45. Trey K. Sato, T.D., Scott D. Emr. Vam7p, a SNAP-25-Like Molecule, and Vam3p, a Syntaxin Homolog, Function Together in Yeast Vacuolar Protein Trafficking. Molecular and Cellular Biology 1998, 18, 5308–5319.
46. Christian Ungermann, W.W. Vam7p, a vacuolar SNAP-25 homolog, is required for SNARE complex integrity and vacuole docking and fusion. The EMBO Journal 1998, 17, 3269–3276.
47. Albert Haas, B.C., William Wickner. G-protein ligands inhibit in vitro reactions of vacuole inheritance. The Journal of Cell Biology 1994, 126, 87-97.
48. Kevin G. Hardwick, H.R.B.P. SED5 encodes a 39-kD integral membrane protein required for vesicular transport between the ER and the Golgi complex. The Journal of Cell Biology 1992, 119, 513-521.
49. David K. Banfield, M.J.L., Hugh R.B. Pelham. A SNARE like protein required for traffic through the Golgi complex. Nature 1995, 375, 806-809.

50. James A. McNew, J.G.S.C., Morten Sogaard, Boris V. Zemelmen, Christian Wimmer, Wanjin Hong, Thomas H. Sollner. Gos1, a saccharomyces SNARE involved in Golgi transport. FEBS Letters 1998, 435, 89-95.
51. Corrado Viotti, J.B., York-Dieter Stierhof, Melanie Krebs, Markus Langhans, Willy van den Berg, Walter van Dongen, Sandra Richter, Niko Geldner, Junpei Takano, Gerd Jurgens, Sacco C. de Vries, David G. Robinson, Karin Schumacher. Endocytic and secretory traffic in Arabidopsis merge in the trans-Golgi network/early endosome, an independent and highly dynamic organelle. The Plant Cell 2010, 22, 1344–1357.
52. Franz Wendler, S.T. Syntaxin 6: The Promiscuous Behaviour of a SNARE Protein. Traffic 2001, 2, 606–611.
53. Anita C. Hohenstein, P.A.R. SNAP-29 Is a Promiscuous Syntaxin-Binding SNARE. Biochemical and Biophysical Research Communications 2001, 285, 167–171.
54. Bin Yang, L.G., Jr., Rytis Prekeris, Martin Steegmaier, Raj J. Advani, Richard H. Scheller. SNARE Interactions Are Not Selective IMPLICATIONS FOR MEMBRANE FUSION SPECIFICITY. THE JOURNAL OF BIOLOGICAL CHEMISTRY 1999, 274, 5649–5653.
55. Marco M. K. Tsui, D.K.B. Yeast Golgi SNARE interactions are promiscuous. Journal of Cell Science 2000, 113, 145-152.
56. Noriko Furukawa, J.M. Multiple and distinct strategies of yeast SNAREs to confer the specificity of membrane fusion. Scientific Reports 2014, 4, 1-13.
57. Sarah E. FLOWERDEW, R.D.B. A VAMP7/Vti1a complex distinguishes a non-conventional traffic route to the cell surface used by KChIP1 and Kv4 potassium channels. Biochem J 2009, 418, 529–540.
58. an G. Ganley , E.E., Suzanne R. Pfeffer. A syntaxin 10-SNARE complex distinguishes two distinct transport routes form endosomes to the trans-Golgi in human cells. The Journal of Cell Biology 2008, 180, 159–172.
59. Eisuke Itakura, C.K.-I., Noboru Mizushima. The hairpin-type tail-anchored SNARE syntaxin 17 targets to autophagosomes for fusion with endosomes/lysosomes. Cell 2012, 151, 1256–1269.
60. Sharon E. Miller, B.M.C., Airlie J. McCoy, Margaret S. Robinson, David J. Owen. A SNARE–adaptor interaction is a new mode of cargo recognition in clathrin-coated vesicles. Nature Letters 2007, 450.
61. Tomohiro Yamaguchi, I.D., Sang-Won Min, Xiaocheng Chen, Josep Rizo, Thomas C. Sudhof. Sly1 binds to Golgi and ER syntaxins via conserved N-terminal peptide motif. Developmental Cell 2002, 2, 295-305.
62. Anna P. Newman, J.S., Susan Ferro-Novick. Members of a group of interacting yeast genes required for transport from the ER to the Golgi. Molecular and Cellular Biology 1990, 10, 3405-3414.
63. Joseph Shim, A.P.N., Susan Ferro-Novick. The BOS1 gene encodes an essential 27-kd putative membrane protein that is required for vesicular transport from the ER to the Golgi complex in yeast. Journal of Cell Biology 1991, 113, 55-64.
64. Deborah J. Sweet, H.R.B.P. The S. cerevisiae SEC20 gene encodes a membrane glycoprotein sorted by the HDEL retrieval system. EMBO Journal 1992, 11, 423-432.

65. Lena Burri, O.V., Claudia A. Doege, Kay Hofmann, Traude Beilharz, James E. Rothman, Thomas H. Sollner, Trevor Lithgow. A SNARE required for retrograde transport to the endoplasmic reticulum. PNAS 2003, 100, 9873-9877.
66. Karin L. Nicholson, M.M., Rebecca B. Miller, Thomas J. Filip, Robert Fairman, Frederick M. Hughson. Regulation of SNARE complex assembly by an N-terminal domain of the t-SNARE Sso1p. Nature Structural Biology 1998, 5, 793-802.
67. Williams, D.C.; Novick, P.J. Analysis of SEC9 suppression reveals a relationship of SNARE function to cell physiology. PLoS One 2009, 4, e5449, doi:10.1371/journal.pone.0005449.
68. Stenmark, H.; Olkkonen, V.M. The Rab GTPase family. Genome Biol 2001, 2, reviews3007.1-reviews3007.7, doi:10.1186/gb-2001-2-5-reviews3007.
69. Stephanie Buvelot Frei, P.B.R., Maria Nussbaum, Benjamin J. Briggs, Monica Calero, Stephanie Janeczko, Andrew D. Regan, Catherine Z. Chen, Yves Barral, Gary R. Whittaker, Ruth N. Collins. Bioinformatic and comparative localization of Rab proteins revelas functional insights into the uncharacterized GTPases Ypt10p and Ypt11p. Molecular and Cellular Biology 2006, 26, 7299–7317.
70. Sogaard, M., Tani K, Ye RR, Geromanos S, Tempst P, Kirchhausen T, Rotheman JE, Sollner T. A Rab protein is required for the assembly of SNARE complexes in the docking of transport vesicles. Cell 1994, 78, 937-948.
71. Frauke Schimmo ller, I.S., Suzanne R. Pfeffer. Rab GTPases, directors of vesicle docking. THE JOURNAL OF BIOLOGICAL CHEMISTRY 1998, 273, 22161–22164.
72. Grote, E.; Novick, P.J. Promiscuity in Rab-SNARE interactions. Mol Biol Cell 1999, 10, 4149-4161, doi:10.1091/mbc.10.12.4149.
73. Lipatova, Z.; Hain, A.U.; Nazarko, V.Y.; Segev, N. Ypt/Rab GTPases: principles learned from yeast. Crit Rev Biochem Mol Biol 2015, 50, 203-211, doi:10.3109/10409238.2015.1014023.
74. Alexandre Soulard, A.C., Suzette Moes, Frederic Schutz, Paul Jeno , Michael N. Hall. The rapamycin-sensitive phosphoproteome reveals that TOR controls protein kinase A toward some but not all substrates. Molecular Biology of the Cell 2010, 21, 3475–3486.
75. Danielle L. Swaney, P.B., Lea Starita, Ailan Guo, John Rush, Stanley Fields, Nevan J. Krogan, Judit Villén. Global analysis of phosphorylation and ubiquitylation cross-talk in protein degradation. Nature Methods 2013, 10.
76. Linial, M. SNARE Proteins—Why So Many, Why So Few? 1997, 69, 1781—1792.
77. Youji Shimazaki, T.-i.N., Akira Omori, Mariko Sekiguchi, Yoichi Kamata, Shunji Kozaki, Masami Takahashi. Phosphorylation of 25-kDa Synaptosome-associated Protein. 1996, 271, 14548–14553.
78. Marash, M.; Gerst, J.E. Phosphorylation of the autoinhibitory domain of the Sso t-SNAREs promotes binding of the Vsm1 SNARE regulator in yeast. Mol Biol Cell 2003, 14, 3114-3125, doi:10.1091/mbc.e02-12-0804.

CHAPTER 2: UNIVERSAL DONOR TEMPLATES FOR MARKER-FREE GENOMIC EDITING IN *SACCHAROMYCES CEREVISIAE* USING CRISPR-CAS9

2.1 Abstract

The budding yeast Saccharomyces cerevisiae is an excellent model organism for studying a variety of critical cellular processes. Traditional methods to knock in or -out at specific yeast loci utilize PCR-based techniques, in which primers containing gene-specific homologies are used to amplify selectable marker cassettes that replace or insert into a gene of interest. These marker cassettes are transformed into yeast and integrated into the genome via homologous recombination. While simple and cost-effective, these methods are limited by marker availability when multiple gene edits are desired. Similarly, multiple gene edits using this traditional approach also increases the likelihood of non-specific recombination events that occur in previous marker regions. More recently, CRISPR-Cas9 technology has introduced methods to edit the yeast genome without the need for selectable markers. Although efficient, this method is hindered by costly reagents and the need to design and test unique multiple guide RNAs and donor templates for each desired edit. In this study, we have combined these two approaches and have developed a highly efficient economical method to edit the yeast genome marker-free. We have designed two universal donor templates that efficiently repair two commonly used selectable markers KanMX6 and His3MX6 when targeted by Cas9. Furthermore, we demonstrate the effectiveness of these new marker-free tools by sequentially ablating PRC1, PEP4 and PRB1, vacuolar proteases typically inactivated prior to many biochemical and membrane trafficking studies using budding yeast.

2.2 Introduction

The budding yeast Saccharomyces cerevisiae remains an important model organism for investigating many important cellular processes, including being used in research on the etiology and pathogenesis of many human diseases [1-4]. Due to the conservation of many yeast proteins and core cellular machinery in mammalian cells, budding yeast continues to be a powerful tool that can be used to study complex interactions on a simplified scale. Over 25 years ago, Saccharomyces cerevisiae was the first eukaryote to have its full genome sequenced, since then PCR-based protocols that incorporate both auxotrophic and drug-resistance selectable markers have been the most common avenue for genome editing in yeast [5-8]. These methods utilize primers that include 40-50 bp of homologous sequence up- and downstream of the target gene ORF and 20-25 bp of selectable marker sequence for amplification. Subsequent PCR products then recombine into the target locus via homologous recombination [5]. These major advancements led to the creation of widely used yeast collections and gave rise to the synthetic genetic array (SGA) era of genomics and high throughput studies using budding yeast [9-12]. While these original methods significantly advanced the field, researchers were limited by the number of available markers that can be used in a single mutant strain, and multiple edits to a single yeast strain increased the likelihood of "marker swapping" events, which occur when a selectable marker replaces another already in the genome from a previous edit, rather than targeting its intended locus due to the similar amplification sequences used in the primers. Methods for marker recycling were developed to overcome this limitation; however, continuous utilization has been shown to

decrease correct integrations and chromosomal rearrangement in the yeast genome [13]. Although new selectable markers and tags have been developed, little effort has been made to directly address these limitations.

Recently, the availability of gene ablation and modification technologies using CRISPR-Cas9 systems have become widely available, and others have successfully applied the tool to budding yeast [14-17]. Thus, genome edits can now be done without the need for selectable markers. These methods target Cas9 to a unique PAM (protospacer-adjacent motif) sequence in the target gene with a "guide RNA" (gRNA) specific to the region to be edited. After recognition of the PAM sequence Cas9 precisely cuts the target locus by creating a double-stranded break. Inclusion of a user-designed "DNA donor template" with homologous sequence integrates into the target gene locus via homologous recombination. While this method is highly efficient, drawbacks include costly reagents and difficulty in designing and testing multiple customizable gRNAs and repair templates for each proposed edit which is likely why these tools have not become standard protocol in research labs.

To ameliorate cost and time-consuming design efforts required for incorporating CRISPR-Cas9 into standard yeast editing protocols, we focused our efforts to improve existing tools. Firstly, we found primer specific regions in common PCR-based gene deletions modules first described by Longtine et al., which can be used as universal donor repair templates for marker-free gene editing when Cas9 is targeted to these selectable markers [5]. Secondly, we found common regions of the BY4741/4742 deletion collection can also be efficiently used as universal repair templates in these collections. We also found that our engineered CRISPR-Cas9 plasmids containing gRNA specific to

either the His3MX6 or KanMX6 work efficiently with the universal donor repair templates and allow for sequential gene edits, thereby bypassing all marker limitations. As a proof of concept, we engineered a marker-free TVY614, a widely utilized yeast strain that contains mutations in vacuolar proteases PRC1, PEP4, PRB1 but has limited usage because of selectable marker availability [18-20]. Taken together, we believe our findings result in a significant improvement in PCR-based gene modifications in yeast and have pending applications to the yeast research and educational communities.

2.3 Materials and Methods

Yeast Growth Conditions and Transformations

All yeast strains were grown at 30°C in YPD unless otherwise noted. All yeast transformations were performed using the lithium acetate method [21]. For CRISPR-Cas9 transformations, carrier ssDNA, Cas9 expression plasmid (250ng), and Donor DNA templates (10μg) were added to cells and incubated for 30 mins at 30°C before heat shock. Cells were grown in standard synthetic complete medium lacking nutrients required to maintain selection for auxotrophic markers and/or plasmid, unless indicated otherwise [22]. Yeast strains were constructed in BY4741/2 (MATa/α his3-1, leu2-0, met15-0, and ura3-0) by homologous recombination of gene-targeted, polymerase chain reaction (PCR)-generated DNAs using the method of [5] and/or derived from the EUROSCARF KanMX deletion collection (Open Biosystems/Thermo Scientific, Waltham, MA) or produced by replacement of the complete reading frame with the URA3 cassette. Gene deletions were confirmed by PCR amplification of the deleted locus. To induce iron starvation, cells were grown to log phase in synthetic media

containing 50μM of bathophenanthrolinedisulfonic acid. Subsequent iron shock was performed by rinsing the cells with water, and with synthetic media before final resuspension in synthetic media containing 500μM Fe (III) ammonium sulfate for 2 hours at 30°C as previously described [23, 24].

Immunoblotting

For quantitative immunoblot analysis of GFP-Snc1 or Ftr1-2xGFP, cells were grown under standard vegetative or iron starvation conditions to OD600 ≈ 0.5, as described above. Typically, 3.0 x 107 cells were harvested by centrifugation and lysed by glass bead agitation in SDS-PAGE sample buffer. 10% polyacrylamide gels were loaded with 5.0 X107 cell equivalents and transferred onto standard 0.45 μm nitrocellulose. Anti-GFP primary mouse monoclonal antibody (1814460, Roche) was diluted 1:2500 and Santa Cruz (sc-2055) goat anti-mouse HRP-conjugated antibody was used at 1:10000. Anti-Pgk1 at 1:5000 (Life Technologies) was used as loading controls. Centromeric GFP-Snc1 [25] plasmid was used in the processing assays. All enhanced chemiluminescence (ECL) blots were development on a Chemidoc-MP (Bio-Rad) and band intensities were quantified using Quantity One 1D analysis software (Bio-Rad)

Plasmids

All CRISPR-Cas9 plasmids were constructed using the MoClo Yeast Toolkit and cloned using GoldenGate assembly [10]. Briefly, each plasmid was constructed using three intermediates: a gRNA intermediate, a Cas9 intermediate, and a “multigene” backbone. Custom short guideRNA (sgRNA) sequences specific for either KanMX6 or

His3MX6 were cloned into pYTK_50 entry vectors containing GFP dropout regions. Subsequent entry vectors were used to construct the sgRNA intermediate plasmid in pYTK_95.

The Cas9 intermediate were obtained from Cas9 derived from pYTK_36 and cloned into the pYTK_95 backbones. The "multigene backbone" was constructed to contain appropriate connecter sequences for final assembly, a GFP dropout region, a URA3 selectable marker, a KanR selectable marker, and a 2μ origin of replication. All three intermediates were recombined via GoldenGate assembly to produce the final Cas9 expression plasmids; pJG01 (His3MX6) and pJG02 (KanMX6).

Donor DNA templates and transformation efficiency

Oligonucleotides for F1-R1and U2-D2 donor DNA templates described in Table 2 were commercially synthesized and purchased from Eurofins Genomics (Louisville, KY). For F1-ADE2-R1 and U2-ADE2-D2 donor DNA templates, full length ADE2 was PCR amplified from genomic DNA with overhangs containing F1 and R1, or U2 and D2 sequences, respectively.

To calculate transformation efficiency, red ade2 mutants were transformed with pJG01 or pJG02 and with associated donor DNA templates. Transformants were grown on selective media containing low 15mg/L adenine. Candidates were scored by the presence of red or white coloration. White colonies were inferred to have successfully been edited by CRISPR-Cas9 and ten candidates were randomly selected for PCR amplification of the deleted locus to confirm correct genomic integration sites.

Light Microscopy and Image Analysis

Yeast cells from cultures grown to OD600 ≈ 0.5 were mounted in growth medium, and 3D image stacks were collected at 0.3-µm z increments on a DeltaVision elite workstation (Cytiva) based on an inverted microscope (IX-70; Olympus) using a 100×1.4NA oil immersion lens. Images were captured at 24°C with a 12-bit charge-coupled device camera (CoolSnap HQ; Photometrics) and deconvolved using the iterative-constrained algorithm and the measured point spread function. Image analysis and preparation was done using Softworx 6.5 (Cytiva) and ImageJ v1.50d (Rasband). To quantify vacuolar lumen localization, wildtype cells or mutants were visually scored for presence of GFP in the vacuolar lumen. GFP-Snc1 and Ftr1-2xGFP vacuolar fluorescence intensities were quantified from z stacks collected at 0.3-µm intervals. A minimum of 100 cells were used in all experimental conditions and performed in biological triplicate.

Table 1. Plasmids used in this study.

Name	Plasmid Marker	Source
pJG-001	Kanamycin/URA3	This Study
pJG-002	Kanamycin/URA3	This Study
pRS315 GFP-SNC1	Ampicillin/LEU2	[25]

Table 2. Oligos used in this study.

Name	Sequence
F1-R1 Donor	CGGATCCCCGGGTTAATTAAGGCGCGCCAGATCTGTTTAGGATACTAACGCCGCCATCCAGTTTAAACGAGCTCGAATTC
U2-D2 Donor	CGTACGCTGCAGGTCGACGGATCCCCGGGTTAATTAAGGCGCCGCCATCCAGTGTCGAAAACGAGCTCGAATTCATCGAT
PRC1-F1	ACTCACTAGAGATTGTTTCTTTTCTACTCAACTTAAAGTATACATACGCTCGGATCCCCGGGTTAATTAA
PRC1-R1	TATATTTCGATCGTAGCTGATAATAAAAACGGTATGCC

	TACACATACACGCTGAATTCGAGCTCGTTTAAAC
PRC1-Seq F	GGGTCTCAAAGAAGGGGCCCACTAATAAAAGC
PRC1-Seq R	GAAGCAGCTCTATTGTTTTCTTTTTTTTTAATG
PEP4-F1	AGTGACCTAGTATTTAATCCAAATAAAATTCAAACAAA AACCAAAACTAACCGGATCCCCGGGTTAATTAA
PEP4-R1	CTCTCTAGATGGCAGAAAAGGATAGGGCGGAGAAGTAA GAAAAGTTTAGCGAATTCGAGCTCGTTTAAAC
PEP4-Seq F	CCTCAATTGTATTTGCTGAGGTC
PEP4-Seq R	TGATCGTACAGAGGGCGATTG
PRB1-F1	AGCTTCATCGCCAATAAAAAAACAAACTAAACCTAATT CTAACAAGCAAAGCGGATCCCCGGGTTAATTAA
PRB1-R1	CTAAGGAAAGAAAAAGAAAAAAAAAAGCAGCTGAAATT TTTCTAAATGAAGAAGAATTCGAGCTCGTTTAAAC
PRB1-Seq F	GGGCTTTCGGCTTTGGAAATTTAGGTGACTT
PRB1-Seq R	TATTTCGCGTACCTAATACATCGTCACCACACAC
PRB1-Ext F	AAAACGAGGGCTGGGAAATG
PRB1-Ext R	TGAGAAGCGGGTCACAAAGG

Table 3. Yeast strains used in this study

Name	Genotype	Source
BY4741	*MAT*a *his3Δ1 leu2Δ0 lys2Δ0 ura3Δ0*	This Study
BY4742	*MATα his3Δ1 leu2Δ0 lys2Δ0 ura3Δ0*	This Study
JGY-17	*MATα his3Δ1 leu2Δ0 lys2Δ0 ura3Δ0 ade2Δ::kanMX6*	[13]
JGY-20	*MATα ade2Δ::His3MX6 leu2Δ0 lys2Δ0 ura3Δ0*	This Study
JGY-21	*MATα his3Δ1 leu2Δ0 lys2Δ0 ura3Δ0 ade2Δ*	This Study
JGY-28	*MAT*a *his3Δ1 leu2Δ0 lys2Δ0 ura3Δ0 ade2Δ*	This Study
JGY-61	*MATα his3Δ1 leu2Δ0 lys2Δ0 ura3Δ0 prb1Δ::kanMX6*	[13]
JGY-614	*MATα his3Δ1 leu2Δ0 lys2Δ0 ura3Δ0 prc1Δ pep4Δ prb1Δ*	This Study
JGY-63	*MATα* FTR1-2xGFP::HIS3 *leu2Δ0 lys2Δ0 ura3Δ0*	This Study
JGY-64	*MATα* FTR1-2xGFP::HIS3 *leu2Δ0 lys2Δ0 ura3Δ0 prc1Δ pep4Δ prb1Δ*	This Study
JGY-65	*MATα* GFP-SNC1 (LEU2) *his3Δ1 lys2Δ0 ura3Δ0*	This Study
JGY-66	*MATα his3Δ1* GFP-SNC1 (LEU2) *lys2Δ0 ura3Δ0 prc1Δ pep4Δ prb1Δ*	This Study
JGY-67	*MATα* GFP-SNC1 (LEU2) *snx4Δ::URA3 his3Δ1 lys2Δ0*	This Study

JGY-68	*MATα his3Δ1* GFP-SNC1 (LEU2) *snx4Δ::URA3 lys2Δ0 prc1Δ pep4Δ prb1Δ*	This Study

Table 4. Primers used to confirm JGY614

Name	Sequence	Expected Size
P1	GGGTCTCAAAGAAGGGGCCCACTAATAAAAGC	Full Length: 2021 bp
P2	GAAGCAGCTCTATTGTTTTCTTTTTTTTTAATG	His3MX6Δ: 1825 bp Marker-free: 502 bp
P3	CCTCAATTGTATTTGCTGAGGTC	Full Length: 2168 bp
P4	TGATCGTACAGAGGGCGATTG	His3MX6Δ: 2353 bp Marker-free: 1030 bp
P5	GGGCTTTCGGCTTTGGAAATTTAGGTGACTT	Full Length: 2472 bp
P6	TATTTCGCGTACCTAATACATCGTCACCACACAC	kanMX6Δ: 2125 bp Marker-free: 646 bp
P7	ACTCACTAGAGATTGTTTCTTTTCTACTCAACT TAAAGTATACATACGCTC GGATCCCCGGGTTA ATTAA	His3MX6:1403 bp
P8	TATATTTCGATCGTAGCTGATAATAAAAACGGT ATGCCTACACATACACGCTGAATTCGAGCTCGT TTAAAC	
P9	AGTGACCTAGTATTTAATCCAAATAAAATTCAA ACAAAAACCAAAACTAACCGGATCCCCGGGTT AATTAA	His3MX6:1403 bp
P10	CTCTCTAGATGGCAGAAAAGGATAGGGCGGAG AAGTAAGAAAAGTTTAGCGAATTCGAGCTCGT TTAAAC	
P11	AAAACGAGGGCTGGGAAATG	*prb1Δ::kanMX6:* 2251 bp
P12	TGAGAAGCGGGTCACAAAGG	

2.4 Results

Marker-free strategy and efficiency

In our study, we demonstrate a significant improvement to existing yeast gene editing tools that utilize PCR-based integrations and CRISPR-Cas9 methodologies. We found our strategy is economical and can efficiently generate marker-free gene edits. Our workflow requires two steps. First, the gene ORF of interest is modified using traditional

PCR-based integration techniques with two of the most common selectable markers (His3MX6 or KanMX6) as first described by Longtine et al., which results in the integration of the selectable marker flanked by F1 up- and R1 downstream sequences [5]. Second, we use optimized gRNAs to target Cas9 to selectable markers His3MX6 (Figure 1A) or KanMX6 (Figure 1B-C). We found our gRNA-Cas9s sufficiently create double-stranded breaks, which promotes efficient replacement of the selectable marker by a single stranded 80 bp concatenated F1-R1 donor oligo (Table 2) via homologous recombination. Similarly, we found the KanMX6 selectable marker in the commercially available BY4742 deletion collection were also flanked by U2 up- and D2 downstream sequences at the sites of integration which can also be targeted by pJG02 and replaced using a single stranded 80 bp concatenated U2-D2 Donor oligo (Table 2) via homologous recombination to produce marker-free genomic modifications [18].

To measure the efficiency of our marker-free strategy, we utilized a red to white screen using ade2 mutants that accumulate purine precursors in the Ade2 biosynthesis pathway which can easily be visualized as red phenotype on low adenine media (15mg/L) [26, 27]. We applied our marker-free strategy on ade2 mutants derived from PCR-based knockouts containing His3MX6 and KanMX6 or an ade2□::kanMX6 obtained from the BY4742 deletion collection (Figure 1). To determine the efficiency of our strategy, we modified the DNA donor templates to include a wildtype copy of the ADE2 gene within each donor template. We found successful replacement of the selectable markers with the ADE2 donor DNA template resulted in the cells restoring ADE2 biosynthesis which ameliorated the red phenotype and returned the cells to white when grown on low adenine media. Using this assay, we determined our F1-R1 donor DNA template

exhibited a high degree of efficiency for both His3MX6 and KanMX6, with 87% and 92% reverting to white, respectively (Figure 2). While the U2-D2 DNA donor repair template was far less efficient, with only 30% of colonies reverting to white (Figure 2).

Creation of a Marker-free Protease Deficient Strain

Next, we sought to determine if the integrated donor DNA templates would prohibit subsequent modifications using repeated marker-free ablations. To test this, we narrowed our focus to generating a useful tool for the yeast research community and decided to apply our strategy by engineering a marker-free protease deficient yeast strain. We found inspiration using TVY614, a well-utilized protease deficient yeast strain commonly used for studying protein overexpression and membrane trafficking first developed by the Emr Lab [20]. In this strain, three major vacuolar proteases Pep4, Prc1 and Prb1 were knocked out using classical yeast genetic manipulations using selectable markers. While the TVY614 strain has been an excellent asset to many research labs for the past 30 years, the strain's limited available selectable markers have long restricted most experiments to just a few genetic modifications. Therefore, we believed a marker-free variant of this strain would be a desirable reagent to the yeast community and successfully engineered the strain using the following steps.

First, we deleted PRC1 with standard PCR-based genomic editing using His3MX6 flanked by F1 and R1 sequences (Figure 3D Lane 4). Next, we transformed these cells with pJG01 and the F1-R1 DNA donor template (Figure 3A). All candidates were PCR verified and grown on 5-FOA to drop out the Cas9 plasmid (Table 4). The procedure was repeated for PEP4 marker-free deletion without incident (Figure 3B).

However, upon repeating the procedure for a third time for the PRB1 locus, we failed to insert a PCR amplified His3MX6 cassette into the gene locus, suggesting multiple F1-R1 sequences in the genome does negatively affect subsequent modifications, likely causing non-specific marker integrations. However, we did eventually find success by amplifying genomic DNA 350 bp up and downstream from the prb1Δ::kanMX6 locus obtained from the BY4742 deletion collection (Figure 3C). We hypothesized the larger amount of homologous sequence combined with the absence of F1-R1 sequence would drive greater specificity during homologous recombination. Indeed, using this strategy we obtained >100 isolates of prc1Δ pep4Δ prb1Δ::kanMX6 which was then targeted for marker removal using JG02 in conjunction with the U2-D2 donor DNA template (Figure 3C). We also found the final selectable marker removal via gRNA-Cas9 was highly efficient and resulted in >100 candidates of which four isolates were confirmed by PCR. We have named the resulting strain JGY614 to acknowledge the clear emulation to the original TVY614 strain (Figure 3E).

To confirm that vacuole proteostasis is impaired in JGY614, we visualized and measured the steady state protein abundance of two well-characterized vacuolar localizing proteins, Snc1 and Ftr1. Snc1 is a v-SNARE that has been shown to traffic to the vacuole through multiple pathways, and Ftr1, an iron transporter that is primarily found on the plasma membrane and is trafficked to the vacuole for degradation upon binding to iron complexes [23, 24, 28-30]. In JGY614, GFP-Snc1 showed clear retention at the plasma membrane and a strong vacuole signal as compared to wildtype cells (Figure 4A). Recently, sorting nexin Snx4 was found to mediate Snc1 trafficking from the vacuole membrane, resulting in increased Snc1 degradation in snx4□ cells [28]. Here

we confirm these results, however when Snx4 is ablated in JGY614, cells exhibited far less vacuole fluorescence intensities and contained many internal compartments indicating multiple trafficking defects are present (Figure 4A). Quantitative immunoblot analysis of steady-state GFP-Snc1 further confirmed the loss of Snc1 degradation in JGY614. GFP-Snc1 was found to be 30% degraded in wildtype cells and 40% degraded in snx4D cells. In JGY614, GFP-Snc1 degradation is reduced to 9% in wildtype and 5% in JGY614 (Figure 4B). Similarly, we localized Ftr1-2xGFP under iron replete conditions which causes rapid processing of Ftr1 as it is trafficked to the vacuole for degradation. After 2 hours in iron replete conditions, Ftr1-2xGFP was retained in the vacuole and plasma membrane in JGY614, while very little fluorescence was present in wildtype cells (Figure 4C). Quantitative immunoblot analysis of steady-state Ftr1-2xGFP found protein abundance was increased 10-fold in JGY614 as compared to wildtype cells, indicating vacuolar proteases are greatly impaired (Figure 4D).

2.5 Discussion

In this study, we have successfully combined traditional PCR-based techniques with CRISPR-Cas9 to create an economical and efficient strategy to edit the yeast genome marker-free. We believe this system satisfactorily addresses many of the drawbacks and limitations that have prevented many yeast research labs from routinely adopting CRISPR-Cas9 protocols in their labs. Firstly, we tested multiple guideRNAs and have optimized two gRNAs that efficiently target Cas9 to His3MX6 or KanMX6, these constructs are available by request. Secondly, we discovered common sequences found in traditional PCR-based techniques used to modify yeast can be used as donor

DNA templates to remove selectable markers in combination with associated gRNA-Cas9 constructs. Therefore, two “universal” donor DNA templates comprising of either F1 and R1 for strains derived by Longtine et al. or U2 and D2 sequences for strains derived from the BY4741/2 deletion collections are required in conjunction with the associated gRNA-Cas9 plasmids. These donor DNA templates are single stranded oligos which can be synthesized commercially at high concentrations for just a few dollars. We especially found markers knocked out using F1-R1 donor DNA templates occurred at a higher efficiency than using the U2-D2 donor DNA templates. Finally, we have demonstrated the ability to sequentially modify and remove selectable markers at least three times during the engineering of our marker-free protease deficient strain, JGY614. In our experience, one to two marker-free modifications can occur at high frequency, however subsequent modifications result in a significant reduction in specificity. Additionally, we suspect that as the number of marker-free modifications accumulates the chances of nonspecific recombination at previously modified loci also increases. In these cases, we suggest increasing flanking homologous sequences and alternating donor DNA templates and selectable markers, if possible. In our experience, we find sequential marker-free editing of 1-2 genes is generally trouble-free, while 3 or more edits is more challenging. Though we have successfully edited 8 loci using sequential edits and do not find any true limitations to the strategy.

We have also made significant efforts to multiplex two or more gRNAs with multiple selectable markers into a single Cas9 plasmid. However, we found all of our multiplexed gRNA-Cas9 plasmids were not nearly as effective as our individual constructs. Others have noted a similar reduction in efficiency and hypothesized Cas9

concentrations maybe rate limiting when split between additional gRNAs, while others have found success targeting up to four different loci with four separate gRNAs expressed on the same CRISPR-Cas9 plasmid [16]. Therefore, future efforts to construct a multiplex Cas9 plasmid that simultaneously targets multiple selectable markers may be achievable.

Taken together, we believe our findings result in a significant improvement in PCR-based gene methodologies in yeast. We believe our strategy can be easily applied to any yeast collection that uses His3MX6 or KanMX6 and has common sequences flanking the selectable markers. Additionally, our gRNA-Cas9 constructs can be used to perform an unlimited number of gene edits, therefore researchers can knockout entire pathways or protein families, faster and cheaper than any other available system. Likewise, we believe this new strategy can easily be adapted as a low cost but effective educational tool to demonstrate CRISPR-Cas9 technology in the classroom.

2.6 Acknowledgements

We are grateful to the members of the Chi Lab and Mandi Ma for thoughtful discussions and comments on this manuscript. We would like to thank undergraduate researchers Alyssa Lucero, Carrie Rapier, Jordan Swaby, and Briggs Yoder for their direct efforts in developing the project. This work was supported by the National Science Foundation 2028519 to RJC and UNC Charlotte Faculty Research Grants Program to RJC.

2.7 Figures

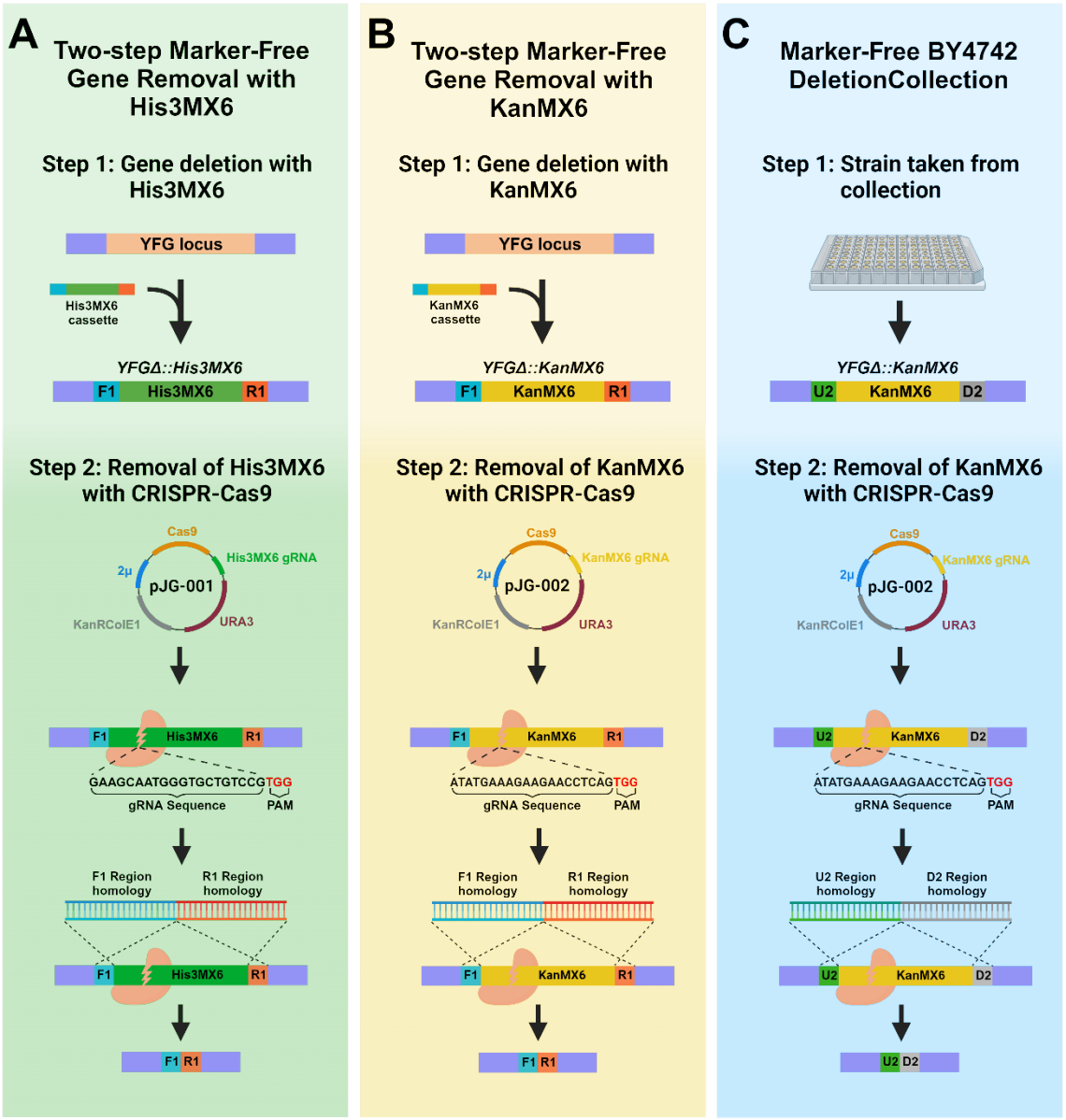

Figure 1. Marker-free genomic editing. Our method uses a combination of traditional gene manipulation techniques using PCR-based selectable markers followed by removal using CRISPR-Cas9. **A-B)** Genes modified using the traditional Longtine et al. technique have residual F1 and R1 sequences located up- and downstream of the selectable marker. Transformation with CRISPR plasmids (pJG01(His3MX6) or pJG02(KanMX6) and the F1-R1 donor repair template results in the removal of the selectable marker. **C)** BY4741/2 deletion collections have residual U2 and D2 sequences located up- and downstream of the KanMX6 selectable marker. Transformation with CRISPR plasmid (pJG02(KanMX6)) and the U2-D2 donor repair template results in the removal of the selectable marker.

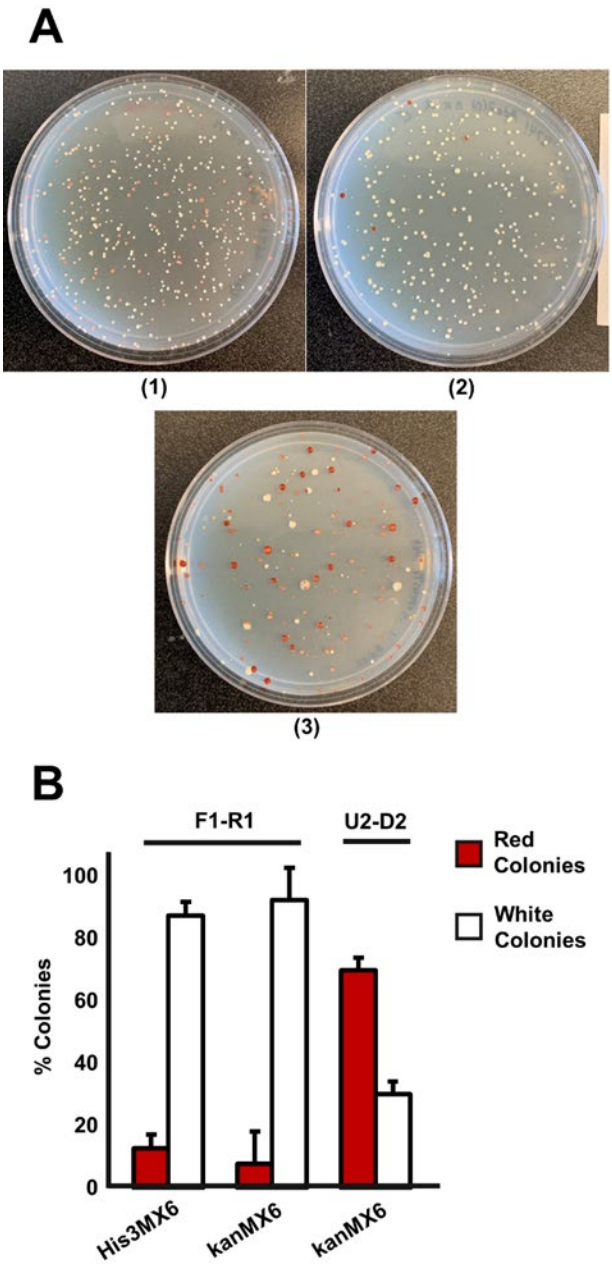

Figure 2. Marker-free transformation efficiency. **A)** Representative plates of F1-ADE2-R1 or U2-ADE2-D2 donor templates transformed into *ade2Δ* strains (pink/red) with indicated Cas9 plasmids. **B)** Transformation efficiency was calculated by the ratio of pink/red to white colonies. F1-ADE2-R1 donor efficiency when targeting HisMX6 and KanMX6 was 80% and 90%, respectively. Transformation efficiency was reduced to 35% when using U2-ADE2-R1 donor repair template in the BY4742 deletion collection.

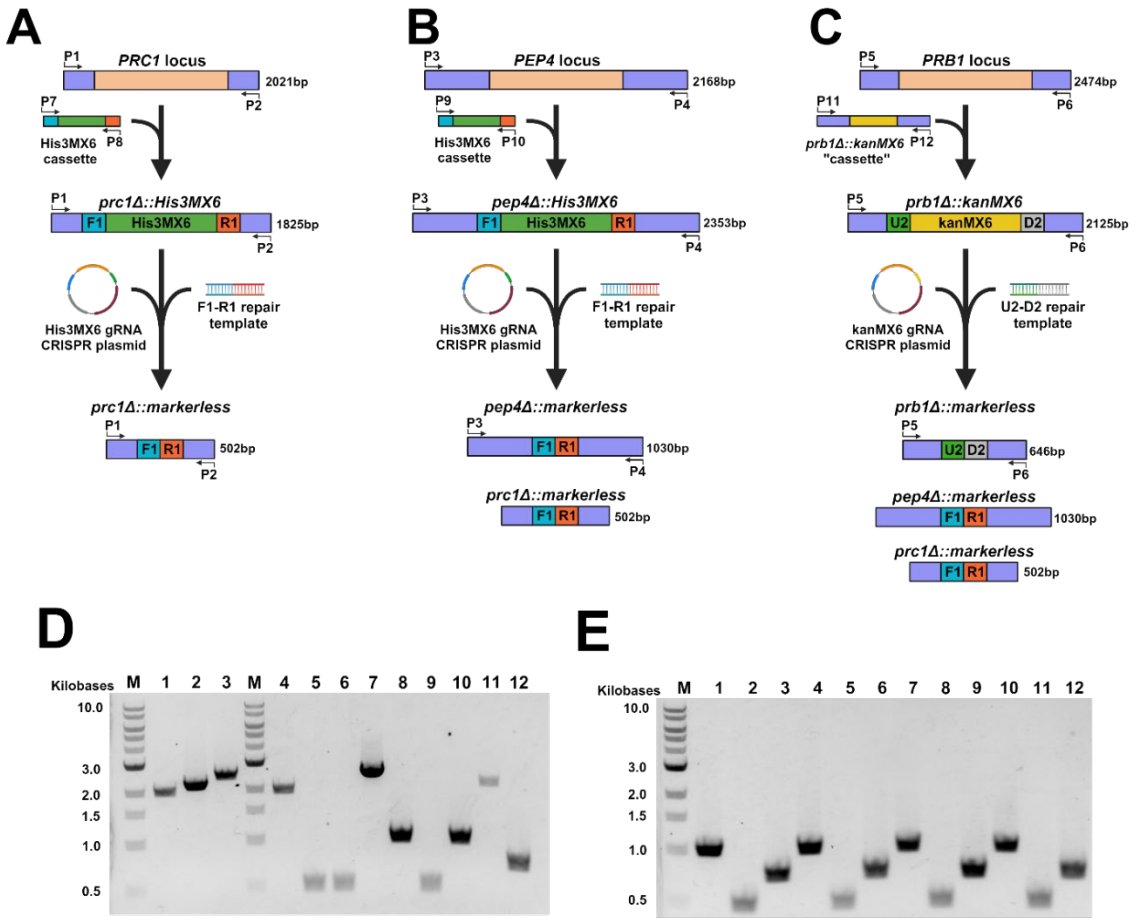

Figure 3. Engineering a marker-free protease deficient strain using sequential marker-free knockouts **A-C)** Vacuolar proteases, Prc1, Pep4 and Prb1 were sequentially targeted for marker-free deletion. PRC1 was knocked out first using standard PCR-based marker techniques, and His3MX6 marker was removed by Cas9 and replaced by the F1-R1 donor repair template. This was followed by Pep4 and then Prb1 sequentially using a similar approach, except KanMX6 was used for Prb1. **D)** PCR using indicated primers (**Table 3**) on genomic DNA was used at each step to confirm each successful genomic integration. Lanes 1-3 bands demonstrate the presence of PRC1, PEP4, PRB1, respectively in our beginning strain. Lane 4 indicates the successful replacement of PRC1 with HisMX6, followed by the removal of the marker by Cas9 as shown in lanes 5-6. Lane 7 indicates the successful replacement of PEP4 with His3MX6, followed by the removal of the marker by Cas9, as shown in lanes 8 and 10 while maintaining the PRC1 locus marker-free shown in lane 9. Lane 11 indicates the successful replacement of PRB1 with KanMX6, followed by the removal of the marker by Cas9 as shown in lanes 12. **E)** Final genotypes of four marker-free isolates of TGY614 MATα *his3Δ1 leu2Δ0 lys2Δ0 ura3Δ0 prc1Δ pep4Δ prb1Δ* were confirmed at the PRC1 locus (lanes 1, 4, 7, 10), PEP4 locus (lanes 2, 5, 8, 11) and PRB1 locus (lanes 3, 6, 9, 12). All primers and expected sizes are described in **Table 4**.

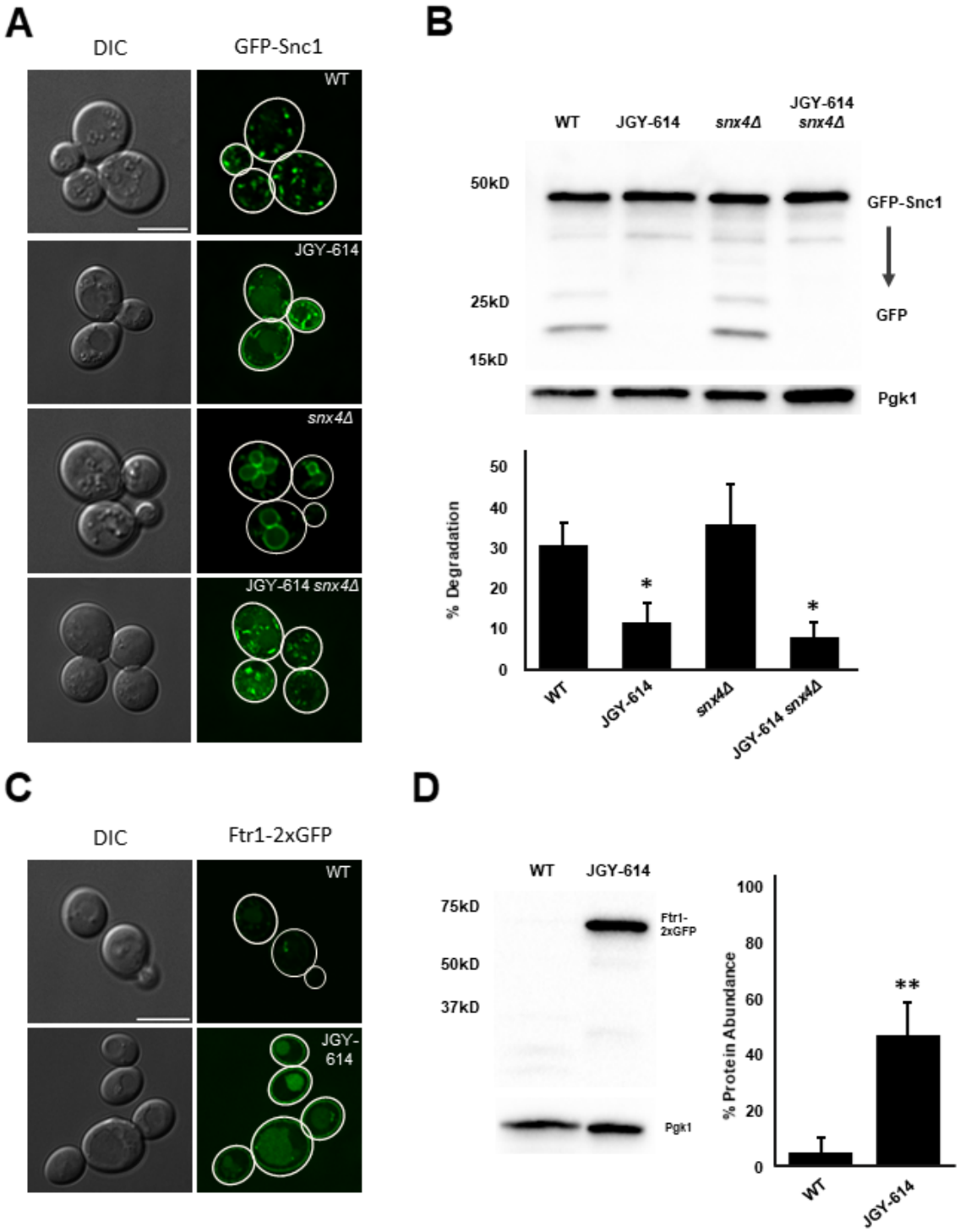

Figure 4. JGY614 vacuole proteostasis is impaired. (**A, C**) Two proteins normally trafficked to the vacuole and degraded were tagged with GFP in wildtype or JGY614 cells. **A)** Micrographs indicate SNARE protein GFP-Snc1 and Ftr1-2xGFP recycles from to and from the plasma membrane via an endo-vacuolar pathway and both GFP signals are enriched in JGY614 backgrounds. **B)** GFP-Snc1 processing assay resulted in a 30% degradation, this is exacerbated to 40% in *snx4Δ* cells. In JGY614, GFP-Snc1

degradation is reduced to 9% and 5%, respectively. Graph values were analyzed via single-factor ANOVA and Tukey HSD, with asterisks representing $p < 0.05$. **D)** Ftr1-GFP processing assay after wildtype and JGY-614 were replete of iron. In wildtype cells, Ftr1-GFP is nearly undetectable by western blot but stabilized in JGY614 cells. Values were analyzed via unpaired T-test, with asterisks representing $p < 0.01$. All scale bars indicate 5µm.

2.8 References

1. D Botstein, G.F., Yeast: an experimental organism for modern biology. Science, 1988. 240: p. 1439-1443.
2. Botstein, D. and G.R. Fink, Yeast: an experimental organism for 21st Century biology. Genetics, 2011. 189(3): p. 695-704.
3. Pereira, C., et al., Contribution of yeast models to neurodegeneration research. J Biomed Biotechnol, 2012. 2012: p. 941232.
4. Shahin Mohammadi, B.S., Shankar Subramaniam, Ananth Grama, Scope and limitations of yeast as a model organism for studying human tissue-specific pathways. BMC Sys Biol, 2015. 9(96).
5. Longtine, M.S., et al., Additional modules for versatile and economical PCR-based gene deletion and modification in Saccharomyces cerevisiae. Yeast, 1998. 14(10): p. 953-61.
6. Bahler, J., et al., Heterologous modules for efficient and versatile PCR-based gene targeting in Schizosaccharomyces pombe. Yeast, 1998. 14(10): p. 943-51.
7. Janke, C., et al., A versatile toolbox for PCR-based tagging of yeast genes: new fluorescent proteins, more markers and promoter substitution cassettes. Yeast, 2004. 21(11): p. 947-62.
8. Sikorski, R.S. and P. Hieter, A system of shuttle vectors and yeast host strains designed for efficient manipulation of DNA in Saccharomyces cerevisiae. Genetics, 1989. 122(1): p. 19-27.
9. Tong, A.H. and C. Boone, Synthetic genetic array analysis in Saccharomyces cerevisiae. Methods Mol Biol, 2006. 313: p. 171-92.
10. Baryshnikova, A., et al., Synthetic genetic array (SGA) analysis in Saccharomyces cerevisiae and Schizosaccharomyces pombe. Methods Enzymol, 2010. 470: p. 145-79.
11. Vizeacoumar, F.J., et al., Integrating high-throughput genetic interaction mapping and high-content screening to explore yeast spindle morphogenesis. J Cell Biol, 2010. 188(1): p. 69-81.
12. Kuzmin, E., et al., Synthetic genetic array analysis for global mapping of genetic networks in yeast. Methods Mol Biol, 2014. 1205: p. 143-68.
13. Akada, R., et al., PCR-mediated seamless gene deletion and marker recycling in Saccharomyces cerevisiae. Yeast, 2006. 23(5): p. 399-405.
14. Akhmetov, A., et al., Single-step Precision Genome Editing in Yeast Using CRISPR-Cas9. Bio Protoc, 2018. 8(6).
15. Adli, M., The CRISPR tool kit for genome editing and beyond. Nat Commun, 2018. 9(1): p. 1911.
16. Lee, M.E., et al., A Highly Characterized Yeast Toolkit for Modular, Multipart Assembly. ACS Synth Biol, 2015. 4(9): p. 975-86.
17. Utomo, J.C., C.L. Hodgins, and D.K. Ro, Multiplex Genome Editing in Yeast by CRISPR/Cas9 - A Potent and Agile Tool to Reconstruct Complex Metabolic Pathways. Front Plant Sci, 2021. 12: p. 719148.
18. Giaever, G. and C. Nislow, The yeast deletion collection: a decade of functional genomics. Genetics, 2014. 197(2): p. 451-65.

19. Giaever, G., et al., Functional profiling of the Saccharomyces cerevisiae genome. Nature, 2002. 418(6896): p. 387-91.
20. Vida, T.A. and S.D. Emr, A new vital stain for visualizing vacuolar membrane dynamics and endocytosis in yeast. J Cell Biol, 1995. 128(5): p. 779-92.
21. Gietz, R.D., et al., Studies on the transformation of intact yeast cells by the LiAc/SS-DNA/PEG procedure. Yeast, 1995. 11(4): p. 355-60.
22. Guide to yeast genetics and molecular biology. Methods Enzymol, 1991. 194: p. 1-863.
23. Strochlic, T.I., et al., Grd19/Snx3p functions as a cargo-specific adapter for retromer-dependent endocytic recycling. J Cell Biol, 2007. 177(1): p. 115-25.
24. Strochlic, T.I., et al., Opposing activities of the Snx3-retromer complex and ESCRT proteins mediate regulated cargo sorting at a common endosome. Mol Biol Cell, 2008. 19(11): p. 4694-706.
25. Shintani, T., et al., Mechanism of cargo selection in the cytoplasm to vacuole targeting pathway. Dev Cell, 2002. 3(6): p. 825-37.
26. Gedvilaite, A. and K. Sasnauskas, Control of the expression of the ADE2 gene of the yeast Saccharomyces cerevisiae. Curr Genet, 1994. 25(6): p. 475-9.
27. Ugolini, S. and C.V. Bruschi, The red/white colony color assay in the yeast Saccharomyces cerevisiae: epistatic growth advantage of white ade8-18, ade2 cells over red ade2 cells. Curr Genet, 1996. 30(6): p. 485-92.
28. Ma, M., C.G. Burd, and R.J. Chi, Distinct complexes of yeast Snx4 family SNX-BARs mediate retrograde trafficking of Snc1 and Atg27. Traffic, 2017. 18(2): p. 134-144.
29. Ma, M. and C.G. Burd, Retrograde trafficking and quality control of yeast synaptobrevin, Snc1, are conferred by its transmembrane domain. Mol Biol Cell, 2019. 30(14): p. 1729-1742.
30. Grissom, J.H., V.A. Segarra, and R.J. Chi, New Perspectives on SNARE Function in the Yeast Minimal Endomembrane System. Genes (Basel), 2020. 11(8).

CHAPTER 3: SNARE PROTEIN EVOLUTION AND EXPANSION DRIVES ENDOSOME COMPLEXITY

3.1 Abstract

The budding yeast Saccharomyces cerevisiae has long been lauded as an excellent model system for studying conserved membrane trafficking pathways in humans such as the secretory pathway and clathrin-mediated endocytosis. However, recent confusion of our fundamental understanding of the yeast endomembrane system has been raised by multiple research groups. Given the vast amount of information that has already been obtained using budding yeast, further studies pertaining to early endocytic uptake and subsequent fusion to primary accepting compartments are greatly needed. Our findings support a prevailing model where the yeast TGNs can act as early and recycling endosomes, rather than involuted distinct structures found in animal cells. In this paradigm, clathrin-coated vesicles invaginate at the plasma membrane, then travel and fuse directly with the Golgi. Cargo is then targeted for degradation from the Golgi to the Pre-vacuolar endosome. In this study, we use molecular, genetic, and evolutionary approaches to understand how Soluble-NSF-Attachment-Receptor (SNARE) evolutionary expansion likely contributed to endosomal complexity in humans. We utilized the spatial dynamics of fluorescent alpha-factor in an internalization screen for endocytic defects using 24 SNARE mutants. In doing so, we have identified Snc1, Snc2, Gos1, Tlg1 and Vti1, as the SNARE machinery that mediates PM vesicle fusion to the TGN. We have also identified the ancestral yeast SNAREs that evolved early/recycling

endosome functions in humans and find heterologous expression in yeast leads to a more complex endosomal system.

3.2 Introduction

For over a century, budding yeast *Saccharomyces cerevisiae* has been used to study a wide range of cellular processes and for the last three decades, has been regarded as one of the best model organisms to study clathrin receptor-mediated endocytosis (CME) and the secretory pathway. CME is a major trafficking pathway that is found in all eukaryotic organisms and is critical for both cell viability and cell signaling [1]. Briefly, cargo first binds to a specific receptor at the plasma membrane (PM), which causes the membrane to bud inwards with the help of clathrin and other adapter proteins. This inward budding eventually forms into a fully enclosed vesicle, which will shed its protein coat before fusing to the primary endocytic accepting organelle, such as the early endosome. The endosomal lumen will gradually acidify as it matures into the late endosome, causing the cargo to dissociate from its receptor. This allows these receptor molecules to be recycled back to the PM via the recycling endosome. The now mature endosome, commonly referred to as the pre-vacuolar endosome (PVE) in yeast, will send material to the lysosome (or vacuole in yeast) for content degradation. Docking of transport vesicles onto correct endomembrane targets is guided by Rab proteins and other tethering factors, while the direct fusion of vesicles to the target membrane is mediated by membrane-bound Soluble-NSF-Attachment-Receptor (SNARE) proteins [2-5].

The classical understanding of the yeast endomembrane system assumed the presence of separate endosomal compartments, however past studies have failed to yield

any protein markers that can be used to distinctly and uniquely label the early/recycling endosomes in budding yeast [6]. Furthermore, researchers have used FM4-64-independent and dependent methods to visualize the yeast endomembrane system. These results suggested that budding yeast lacks a distinct early and recycling endosome, with the TGN acting in place of both of these structures [7]. This suggested a new paradigm where clathrin-coated vesicles are formed by the inward budding of the PM, then travel and fuse directly to the Golgi where receptors are recycled back to the PM via Golgi-derived vesicles. The cargo is then targeted for degradation from the Golgi to the PVE, which sits near the vacuole and acts as a late endosome, sending material for degradation to the vacuole via vesicle formation/fusion. However more recently, others have provided evidence for post-endocytic recycling of nutrient transporters that are mediated by yeast early endosomes, directly challenging this paradigm shift [8]. Given the vast amount of information that has already been obtained using budding yeast, further studies pertaining to early endocytic uptake and subsequent fusion to primary accepting compartments are greatly needed.

We believe understanding SNARE protein family evolution and expansion provides clarity to these new models [9]. SNARE proteins are known to localize and mediate vesicle fusion events with specific membranes and because of this they are perhaps the most well-suited protein family to define the yeast endomembrane system [10]. These proteins contain a conserved SNARE motif and are C-terminally anchored to organelle membranes (or in some cases maintained on membranes through posttranslational modifications), and generally operate in groups of 4 to facilitate fusion of vesicles to the target membrane on which they are located [3, 9, 11-13]. These SNARE

tetramers are referred to as SNAREpins and are comprised of 3 target membrane SNAREs (t-SNAREs) and 1 vesicle membrane SNARE (v-SNARE) [10, 14]. Briefly, the SNAREpin formation occurs once a vesicle reaches its target membrane. The v-SNARE and appropriate t-SNAREs are arranged into position by tethering factors and will form into a coiled-coil structure, allowing short-range docking of the vesicle to its target. The SNARE motif is then "zippered" from N- to C-terminus, acting as a catalyst for membrane fusion by bringing the vesicle and its target into close enough proximity for the generation of a fusion pore [15, 16]. After fusion, the SNAREpin is dissembled by the ATPase NSF and α-SNAP [10, 17]. While all yeast SNAREs have been annotated, interestingly none have been identified to mediate the fusion of plasma membrane-derived vesicles to the TGN [2, 3, 14, 18].

In this study, we use a molecular phylogenetic approach to better understand the evolutionary history of SNARE proteins across eukaryotic evolution. Using this method, we found a clear association between the expansion of yeast Golgi and endosome-associated SNAREs with the rise of early and recycling endosomes compartments during metazoan evolution [19]. In vivo studies using nine heterologously expressed human SNARE proteins in yeast further supports this notion by significantly increasing endosome complexity. Furthermore, we developed a fluorescent α-factor uptake screen and have identified the SNARE fusion machinery that mediates early endocytic vesicle fusion to the TGN.

3.3 Materials and Methods

Phylogenetic Analysis

Full-length sequences for all taxa gene families were aligned with Muscle 3.6 and edited manually in the cases of clear errors [20]. Maximum likelihood analyses were conducted with RAxML v.8.2.4 using a LG+G matrix model determined by ProtTest v.3, and a trimmed alignment containing the SNARE domain [21] [22]. Support for specific nodes for maximum likelihood analyses was assessed with 1,000 bootstraps. Trees were visualized and illustrated with FigTree v1.4 (http://tree.bio.ed.ac.uk/software/figtree/) and were simplified by collapsing branches of homologous SNARE proteins.

Yeast Strains, Growth Conditions and Transformations

All yeast strains were grown at 30°C in YPD unless otherwise noted. All yeast transformations were performed using the lithium acetate method [23]. For CRISPR-Cas9 transformations, carrier ssDNA, Cas9 expression plasmid (250ng), and Donor DNA templates (10μg) were added to cells and incubated for 30 mins at 30°C before heat shock. Cells were grown in standard synthetic complete medium lacking nutrients required to maintain selection for auxotrophic markers and/or plasmid, unless indicated otherwise [24]. Yeast strains were constructed in BY4741/2 (MATa/α his3-1, leu2-0, met15-0, and ura3-0) unless otherwise noted by homologous recombination of gene-targeted, polymerase chain reaction (PCR)-generated DNAs using the method of [25] and/or derived from the EUROSCARF KanMX deletion collection (Open Biosystems/Thermo Scientific, Waltham, MA) or produced by replacement of the complete reading frame with the URA3 or LEU cassette [25]. All gene deletions were confirmed by PCR amplification of the deleted locus. For all FITC α-factor uptake

experiments, proteinase Bar1 was knocked out to increase response sensitivity to α-factor uptake and thus is noted as wildtype when compared to mutant strains.

For inviable SNARE mutants, the auxin-inducible degron system was used to create "conditional nulls" that degrade proteins of interest within 5 minutes of adding the plant hormone auxin to cell media [26, 27]. The TIR1 gene from Oryza sativa was integrated into a DL100 bar1Δ background via linearized expression plasmid containing the TIR1 ORF and a URA3 yeast marker. The plasmid was linearized in the URA3 region, allowing for integration of TIR1 and URA3 in the ura 3-52 locus through homologous recombination [27]. Vital SNAREs of interest were then tagged at the N-terminus with a degron tag, and degradation of each SNARE was observed after addition of auxin via immunoblot. These "conditional null" mutants were then used in α-factor assays by adding room temperature CSM media containing 500 μM indole-3 acetic acid (auxin) after incubation on ice for 2 hours to induce protein degradation.

Plasmids

pJG01 CRISPR-Cas9 plasmid was constructed using the MoClo Yeast Toolkit and cloned using GoldenGate assembly [28]. Briefly, the plasmid was constructed using three intermediates: a gRNA intermediate, a Cas9 intermediate, and a "multigene" backbone. Custom short guideRNA (sgRNA) sequence specific for His3MX6 was cloned into pYTK_50 entry vectors containing GFP dropout regions. The subsequent entry vector was used to construct the sgRNA intermediate plasmid in pYTK_95. The Cas9 intermediate were obtained from Cas9 derived from pYTK_36 and cloned into the pYTK_95 backbones. The "multigene backbone" was constructed to contain appropriate

connecter sequences for final assembly, a GFP dropout region, a URA3 selectable marker, a KanR selectable marker, and a 2μ origin of replication. All three intermediates were recombined via GoldenGate assembly to produce the final Cas9 expression plasmid, pJG01 (His3MX6).

Human SNARE expression plasmids were also constructed using the MoClo Yeast Toolkit and cloned using GoldenGate assembly [28]. Briefly, cDNA from Homo sapiens were purchased from GenScript and each cloned into the YTK_01 entry vector using BsmBI restriction digest and reassembled with T4 DNA ligase. These entry vectors were used to construct "intermediate vectors" containing the yeast PGK1 promoter and terminator sequences and appropriate assembly connectors for final vector construction by cloning into the provided YTK_95 backbone via BsaI assembly. These intermediate vectors were then cloned into 2 final expression plasmids, containing either a URA3 or HIS3 yeast marker, a 2μ origin, and a KanR bacterial marker via BsmBI assembly.

Light Microscopy and Image Analysis

Yeast cells from cultures grown to OD600 ≈ 0.5 were mounted in growth medium, and 3D image stacks were collected at 0.3-μm z increments on a DeltaVision elite workstation (Cytiva) based on an inverted microscope (IX-70; Olympus) using a 100×1.4NA oil immersion lens. Images were captured at 24°C with a 12-bit charge-coupled device camera (CoolSnap HQ; Photometrics) and deconvolved using the iterative-constrained algorithm and the measured point spread function. Image analysis and preparation was done using Softworx 6.5 (Cytiva) and ImageJ v1.50d (Rasband). For FITC α-Factor uptake assays, cell cultures were grown in 5 mL YPD media to log

phase. Cells were washed and resuspended in 50 µL SM minimal media containing 1% BSA and 0.01 mg/mL α-factor conjugated to the FITC (ThermoFisher). Cells were incubated on ice for two hours and centrifuged at 4°C. Cells were then washed three times with 700 µL of SM minimal media (1% BSA) and then resuspended in 50 µL of cold complete synthetic media (CSMD). To obtain images at the time point of zero minutes, the cells were resuspended in 50 µL of SM minimal media (1% BSA) following the washing step and then immediately imaged. To quantify α-factor uptake, a minimum of 100 cells were analyzed for each strain and repeated in triplicate. Wildtype cells or mutants were visually scored for presence of internal fluorescent puncta from z stacks collected at 0.3-µm intervals. Each mutant was compared to wildtype cells via single-factor ANOVA analysis. All experimental conditions were performed in biological triplicate.

Table 1. Yeast strains used in this study.

Name	Genotype	Source
BY4741	*MAT*a *his3Δ1 leu2Δ0 lys2Δ0 ura3Δ0*	This Study
DL100	*MATa* EG123 *ura3-52 leu 2-3,112 trp1-1 his4 can1^{r}*	This Study
HWY2	*MAT*a *bar1Δ::URA3 his3Δ1 leu2Δ0 lys2Δ0*	This Study
HWY11	*MAT*a *bar1Δ::URA3 snc1Δ::HIS3 leu2Δ0 lys2Δ0*	This Study
HWY12	*MAT*a *bar1Δ::URA3 snc2Δ::HIS3 leu2Δ0 lys2Δ0*	This Study
HWY13	*MAT*a *bar1Δ::URA3 vam3Δ::HIS3 leu2Δ0 lys2Δ0*	This Study
HWY16	*MAT*a *bar1Δ::URA3 sso1Δ::HIS3 leu2Δ0 lys2Δ0*	This Study
HWY17	*MAT*a *bar1Δ::URA3 sso2Δ::HIS3 leu2Δ0 lys2Δ0*	This Study
HWY18	*MAT*a *bar1Δ::URA3 gos1Δ::HIS3 leu2Δ0 lys2Δ0*	This Study
HWY22	*MAT*a *bar1Δ::URA3 nyv1Δ::HIS3 leu2Δ0 lys2Δ0*	This Study
HWY23	*MAT*a *bar1Δ::URA3 vam7Δ::HIS3 leu2Δ0 lys2Δ0*	This Study
HWY24	*MAT*a *bar1Δ::URA3 syn8Δ::HIS3 leu2Δ0 lys2Δ0*	This Study
HWY25	*MAT*a *bar1Δ::URA3 spo20Δ::HIS3 leu2Δ0 lys2Δ0*	This Study

HWY26	*MAT*a *bar1Δ::URA3 sec22Δ::HIS3 leu2Δ0 lys2Δ0*	This Study
HWY27	*MAT*a *bar1Δ::URA3 tlg2Δ::HIS3 leu2Δ0 lys2Δ0*	This Study
HWY28	*MAT*a *bar1Δ::URA3 pep12Δ::HIS3 leu2Δ0 lys2Δ0*	This Study
HWY33	*MAT*a *bar1Δ::URA3 vrp1Δ::HIS3 leu2Δ0 lys2Δ0*	This Study
HWY39	*MAT*a *bar1Δ::URA3 his3Δ1 leu2Δ0 lys2Δ0* SLA1-GFP-kanMX6	This Study
HWY35	*MAT*a *bar1Δ::URA3 snc1Δ::HIS3 leu2Δ0 lys2Δ0* SLA1-GFP-kanMX6	This Study
HWY36	*MAT*a *bar1Δ::URA3 snc2Δ::HIS3 leu2Δ0 lys2Δ0* SLA1-GFP-kanMX6	This Study
HWY37	*MAT*a *bar1Δ::URA3 gos1Δ::HIS3 leu2Δ0 lys2Δ0* SLA1-GFP-kanMX6	This Study
JGY4	*MAT*a *bar1Δ::URA3* SEC7-mKate-kanMX6 *his3Δ1 leu2Δ0 lys2Δ0*	This Study
JGY10	*MAT*a *bar1Δ::URA3* VPS5-2xRFP-kanMX6 *his3Δ1 leu2Δ0 lys2Δ0*	This Study
JGY23	*MATa* EG123 *bar1Δ::TRP1 ura3-52 leu 2-3,112 his4 can1^r*	This Study
JGY29	*MATa* EG123 *bar1Δ::TRP1* OsTIR1-URA3 TLG1-deg-kanMX6 *leu 2-3,112 his4 can1^r*	This Study
JGY30	*MATa* EG123 *bar1Δ::TRP1* OsTIR1-URA3 SED5-deg-kanMX6 *leu 2-3,112 his4 can1^r*	This Study
JGY31	*MATa* EG123 *bar1Δ::TRP1* OsTIR1-URA3 VTI1-deg-kanMX6 *leu 2-3,112 his4 can1^r*	This Study
JGY45	*MATa* EG123 *bar1Δ::TRP1* OsTIR1-URA3 SEC9-deg-kanMX6 *leu 2-3,112 his4 can1^r*	This Study
JGY46	*MATa* EG123 *bar1Δ::TRP1* OsTIR1-URA3 SEC20-deg-kanMX6 *leu 2-3,112 his4 can1^r*	This Study
JGY47	*MATa* EG123 *bar1Δ::TRP1* OsTIR1-URA3 UFE1-deg-kanMX6 *leu 2-3,112 his4 can1^r*	This Study
JGY48	*MATa* EG123 *bar1Δ::TRP1* OsTIR1-URA3 SLT1-deg-kanMX6 *leu 2-3,112 his4 can1^r*	This Study
JGY50	*MATa* EG123 *bar1Δ::TRP1* OsTIR1-URA3 *leu 2-3,112 his4 can1^r*	This Study
JGY68	*MATa bar1Δ* SEC7-mKate-kanMX6 *leu2Δ0 lys2Δ0*	This Study
JGY69	*MATa bar1Δ* VPS5-mKate-kanMX6 *leu2Δ0 lys2Δ0*	This Study

Table 2. Plasmids used in this study.

Name	ORF(s)	Selectable Markers	Source
pJG-001	Cas9, His3MX6 gRNA	URA3, KanR	This Study
pJG-003	HsStx7, HsStx8, HsStx12, HsVamp4	URA3, KanR	This Study
pJG-004	HsStx6, HsVamp7, HsVamp8, HsVti1A, HsVti1B	HIS3, KanR	This Study

3.4 Results

Fungi SNAREs have undergone multiple gene duplications and have expanded functions in Metazoans

Using a bioinformatic approach we found the number of SNARE proteins across all eukaryotes widely varied and typically increased as organisms evolved into late metazoans. For example, budding yeast has 24 SNARE proteins while humans have approximately 44. Indeed, others have found SNAREs associated with endosomes duplicated twice across metazoan evolution; first at the transition to multicellularity, and again during the rise of vertebrates, using the choanoflagellates Monosiga brevicola and Monosiga ovata as a representation of the unicellular ancestor to metazoans [19, 29, 30]. We hypothesized SNARE expansion may directly correlate with endosome complexity. Using a similar phylogenetic analysis focusing on endomembrane-associated t-SNAREs and v-SNAREs and using Saccharomyces cerevisiae as a representation of a unicellular ancestor, we found homologs of PVE t-SNAREs in yeast have significantly expanded multiple times across metazoan history, while TGN t-SNARE homologs remained as singletons (Figure 1). Interestingly, we found yeast v-SNAREs Snc1, Snc2, and Nyv1 which predominately localize to PVE structures, to have incurred significant expansion

across metazoan evolution while Ykt6 which is loosely associated with both TGN and PVE structures to not have expanded (Figure 1).

To better understand how the evolution and expansion of these SNARE proteins may have influenced metazoan endosomal system complexity, we further examined the localization of each ancestral yeast SNARE protein in human cells. Using prior published studies and GO term annotations, we found most TGN t-SNARE yeast homologs remained localized to Golgi membranes in human cells, except for Tlg1 which appears to have evolved additional roles at early endosomes (Figure 2A). Interestingly, all PVE t-SNARE yeast homologs have been distributed across the Golgi and early/late endosomal systems (Figure 2A). Similarly, we found that the wide distribution of v-SNARE yeast homologs in the endosomal system suggests they have evolved multiple functions in human cells, except for Sec22 which has retained its primary function at the Golgi throughout metazoan evolution (Figure 2B). Taken together, our results suggest SNARE proteins that evolved early endosome functions in metazoans likely form the SNAREpins responsible for mediating PM vesicle fusion to a primary accepting membrane such as the TGN in yeast. Using this rationale, we prioritized SNARE mutants with early endosome functions to screen for endocytic defects, with the goal of identifying post-endocytic fusion machinery.

FITC α-factor traffics through the minimal endomembrane system in yeast

Fluorescent yeast mating pheromone α-factor has previously been shown to be an excellent tool to study the endocytic pathway in budding yeast by binding to the cell surface receptor Ste2 of Mat a cells [31] and traveling unidirectionally to the vacuole for

degradation [7, 32]. Therefore, we sought to utilize this tool to visualize the primary accepting organelle of PM-derived vesicles in budding yeast. We conjugated α-factor to FITC using a flexible, hydrophilic polyethylene glycol cross-linker and found it maintained functionality comparable to unlabeled α-factor in a dose-dependent Schmooing efficiency assay (data not shown). As others have shown, fluorescent α-factor accumulates on the plasma membrane, internalizes, and fuses to a primary accepting membrane and is degraded in the vacuole within 30 min of triggering endocytosis (Figure 3) [7, 32]. Interestingly, we also colocalized FITC α-factor with Sec7-mKate a marker for the TGN, and Vps5-mKate a marker for the PVE and found our FITC α-factor colocalized with the Sec7-mKate within the first 5 minutes of internalization, then exits and reappears to colocalize with Vps5-mKate after 10 minutes of internalization (Figure 3). These results support a minimal endomembrane model proposed by Day et al [7], where the TGN acts as the primary accepting membrane in yeast and is later degraded via the endo-vacuolar system.

FITC α-factor uptake screen identifies Snc1, Snc2, Gos1, Tlg1, and Vti1 as PM to Golgi SNAREs

Next, we sought to utilize FITC α-factor internalization to determine which SNAREs facilitate PM vesicle fusion to the TGN. Through our phylogenetic analysis, we were able to systematically test FITC α-factor uptake in single SNARE knockouts which are implicated in early endosome function. We hypothesized that the loss of SNARE function at the TGN would result in the loss of fluorescent internal puncta which would indicate participation in the fusion machinery. As predicted, we found significant

endocytic defects in genes associated with early endosomes in metazoans such as SNC1 and SNC2, which are functionally redundant paralog v-SNAREs, which have been reported to facilitate the fusion of PM vesicles [33-35]. To test the eight essential SNARES, we used the auxin-inducible degron system. This system has been shown to successfully target auxin to degron-tagged proteins for degradation, thus creating "conditional deletions" [26, 27]. Using this system, we further identified Tlg1 and Vti1 to be important for FITC α-factor internalization (Figure 4). Consistent with Snc1/2, Tlg1 and Vti1 are t-SNAREs that localized to early endosomes in human cells [7, 36-38]. Upon screening the remaining 12 SNAREs in yeast, we found Gos1, a t-SNARE that primarily localized to the TGN membrane, to be the most critical SNARE for FITC α-factor uptake with a 2-fold reduction, similar to *vrp1*Δ cells, which inhibits internalization at the plasma membrane [39-41]. Taken together, Snc1, Snc2, Gos1, Tlg1, and Vti1 participate in essential SNAREpin formation at the TGN.

Heterologous expression of human SNAREs increases endosome complexity.

While our results indicate a clear association between SNARE protein evolution and the expansion of the endosomal system in humans, it was unclear if the driving force for endosome complexity was due to other factors such as the increase of diverse cargos or other protein families. Interestingly, a study examining organelle generation using computational modeling showed that SNARE proteins could be the basic principle responsible for the biogenesis of distinct cellular compartments [42]. Therefore, we next investigated if the heterologous expression of human SNAREs could drive de novo synthesis of internal organelles in yeast. Others have also shown that human SNAREs

can colocalize with their yeast homologs and even rescue SNARE deletion phenotypes [33, 43].

To test this, we heterologously expressed nine human SNAREs in budding yeast. These include t-SNAREs; Stx6, Stx7, Stx8, Stx12, Vti1A, Vti1B and v-SNAREs; Vamp4, Vamp7, Vamp8, each were chosen because of their direct relatedness to yeast homologs and have been shown to localize to the early endosome, recycling endosome, late endosome, or TGN in humans [44-55]. These SNAREs were expressed in combination as multigene vectors as described in the materials and methods. We again used FITC α-factor to visualize internal compartments upon internalization. Wildtype cells typically had between 1-2 internal fluorescent puncta after 15 min of internalization, however the number increases 1.5-fold if multigene vectors pJG02 (HsStx7, HsStx8, HsStx12, HsVamp4) or pJG03 (HsStx6, HsVamp7, HsVamp8, HsVti1A, HsVti1B) was expressed. Interestingly, we saw an additive effect when simultaneously expressing all 9 SNARE proteins which resulted in a 2-fold increase in internal fluorescent compartments (Figure 5A, C left graph). To identify these new internal fluorescent compartments, we expressed the humans SNAREs with Golgi marker Sec7-mKate and PVE marker Vps5-mKate. While there was no increase in Golgi puncta, there was a 4-fold increase in PVE puncta, suggesting the de novo synthesis of PVE structures is mediated in part by SNARE expression. Overall, our results indicate SNARE protein expansion and expression can drive the generation of more endosomes in yeast and could be the fundamental principle responsible for increasing endosome complexity in late metazoans [42].

3.5 Discussion

For the past few years, there has been considerable confusion with defining the fundamental ultrastructure of the endocytic system in buddying yeast. Some studies have revealed that the yeast endosomal system is much more streamlined than that of mammalian cells with the TGN acting as the primary accepting organelle rather than the early endosome, while others have found independent early/recycling endosome pathways that are cargo specific [8]. Such contradicting studies highlight the need to reexamine the pathways associated with endocytic events post-internalization.

To this extent, no SNARE proteins have been identified to mediate post-endocytic fusion to a primary accepting membrane in yeast. We analyzed the sequences of all 44 human SNAREs and identified the ancestral yeast SNAREs that evolved functions at the early endosome in metazoans. This led us to determine the SNARE proteins responsible for mediating PM vesicle fusion and to identify the primary accepting organelle. Using a fluorescent α-factor internalization assay, we found mutants in three t-SNAREs; Gos1, Tlg1, Vti1 and two v-SNAREs; Snc1/2 had defects in post-endocytic fusion, though had no detectable defects in clathrin coat formation or vesicle invagination. Likewise, complementation of each mutant with ectopically expressed SNAREs plasmids, rescued fluorescent α-factor trafficking to the vacuole, indicating secondary suppressors were not present.

We also measured spatial dynamics of our fluorescent α-factor which first colocalized with TGN marker Sec7, which supports a minimal endomembrane model described by Day et al [7] and identifies TGN as the primary accepting organelle of PM-derived vesicles [7]. We also found when co-expressing nine endosomal-associated

SNAREs from Homo sapiens in yeast, the number of internalized fluorescent α-factor puncta doubled, while the number of PVEs quadrupled, suggesting that additional SNARE proteins contribute to PVE biogenesis. Others have shown that SNARE function is highly conserved and human SNAREs localize to the same membranes as their homologs [33, 43]. This is likely driven by preferential interactions with coat proteins involved in vesicle formation using conserved binding motifs. SNAREs work in tandem with Rabs and other vesicle coat proteins such as COPI and COPII to facilitate membrane fusion [56-58]. Importantly, COPII has been shown to preferentially bind Golgi SNARE proteins through interactions with the SNARE motif, and a recent study found yeast PVE SNARE Syn8 is a retromer cargo [59, 60].

Our findings also complement a study using computational modeling that examined the role of SNARE proteins in organelle biogenesis [42]. Using this mathematical model, researchers found that in order for distinct, separate compartments to exist in a system, they must be in a nonuniform steady state, only possible by each compartment accumulating cognate SNAREs that can pair with one another [42]. Therefore, simply increasing SNARE frequency would not result in the generation of distinct compartments, rather new compartments would only exist as distinct SNARE interactions are introduced. We believe by introducing human t-SNAREs; Stx6, Stx7, Stx8, Stx12, Vti1A, Vti1B and v-SNAREs; Vamp4, Vamp7, Vamp8, we have effectively tripled the number of cognate SNAREs at the endosome in yeast, thus artificially evolving the endosome's complexity.

Furthermore, we believe this is also supported by our phylogenetic analysis of SNARE expansion in metazoans. While Golgi-associated SNAREs have largely

remained unchanged throughout metazoan evolution, endosomal SNAREs comprise the majority of the first of two SNARE expansions- positing that cell polarization may have provided necessary conditions for endosomal SNARE adaptations [19]. This is particularly interesting because SNAREs are known to promiscuously bind, with both cognate and non-cognate SNARE complexes facilitating lipid membrane fusion [61, 62]. However, we found homologs of yeast PVE SNAREs, but not those found on the TGN, evolved early endosome functions in vertebrates. This suggests that the specific expansion of yeast PVE SNAREs may have contributed to the generation of distinct endosomal compartments in metazoans, circumventing the TGN's role as the primary accepting organelle of PM-derived vesicles in budding yeast. However, our model does not preclude the possibility that during the rise of multicellularity came the need for more complex endocytic compartments, necessitated by more stringent endocytic sorting mechanisms. Rather it is more likely that the complexity of modern endosomal systems arose concomitantly with the onset of differential cells and cargoes, while SNARE protein expansion arose to accommodate this increase in capacity. However, more work is needed in early branching metazoans to address this fundamental idea.

3.6 Acknowledgements

We are grateful to the members of the Chi Lab and Dr. Mandi Ma for thoughtful discussions and comments on this manuscript. We would like to thank undergraduate researchers Sarah Cathrine Pascal and Sarah Moody for their direct efforts in developing the project. This work was supported by the National Science Foundation 2028519 to RJC and UNC Charlotte Faculty Research Grants Program to RJC.

3.7 Figures

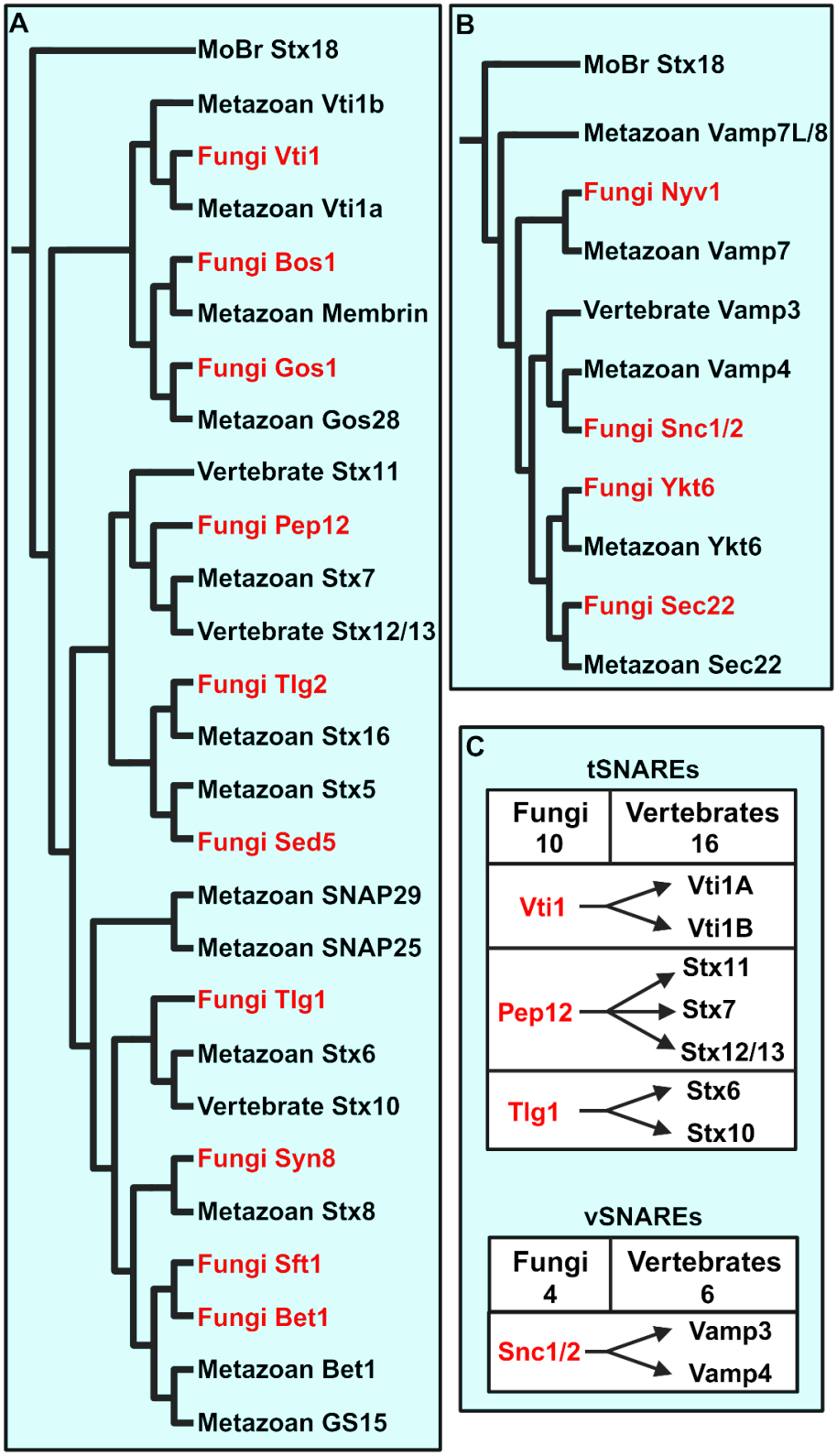

Figure 1. Endosome and Golgi associated SNARE expansion from Fungi to early-late Metazoans. Maximum likelihood analyses of indicated SNARE domains sequences were

analyzed by RAxML. Summary phylogenetic trees demonstrate an expansion of fungi t-SNARE and v-SNARE proteins during eukaryotic evolution. **(A)** Phylogenetic tree of endosome and Golgi associated t-SNARE proteins. **(B)** Phylogenetic tree of endosome and Golgi associated v-SNARE proteins. The ER-associated Syntaxin 18 from Monosiga brevicolisi included as an outgroup. Red lettering indicates fungi SNARE proteins, black lettering indicates metazoan expansion. **(C)** In total, 10 t-SNAREs and 4 v-SNARE proteins in Fungi have been expanded to 16 and 6 in humans, respectively.

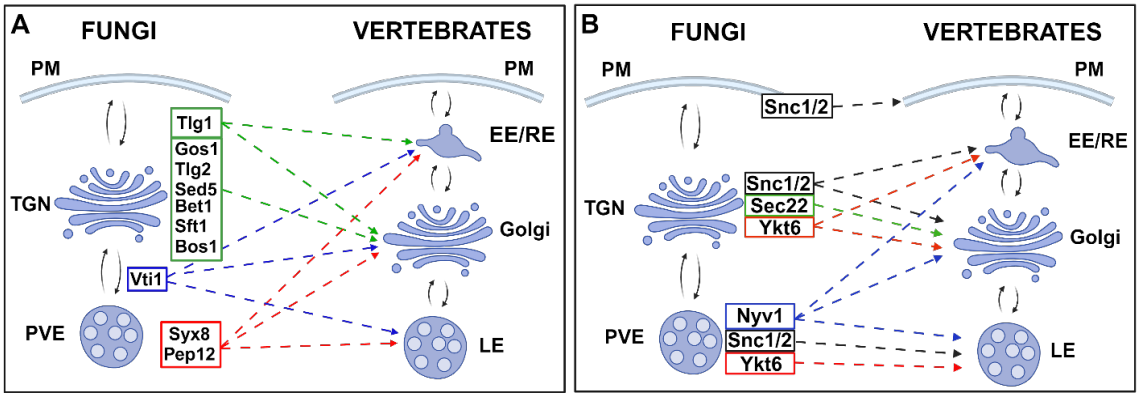

Figure 2. Yeast SNARE homologs have expanded functions in humans. Yeast SNAREs involved in endocytic and Golgi trafficking are denoted by colored boxes (black: PM, green: TGN, blue: TGN and pre-vacuolar endosome, red: pre-vacuolar endosome). Arrows indicate the location of homologous human SNAREs. **(A-B)** While t-SNAREs and v-SNAREs derived from the Golgi have generally remained in Golgi specific, Tlg1, Snc1, Snc2, Ykt6 have been found redistributed to the early endosome along with PVE SNAREs Syx8 and Nyv1. Illustrations in this figure were created with BioRender.

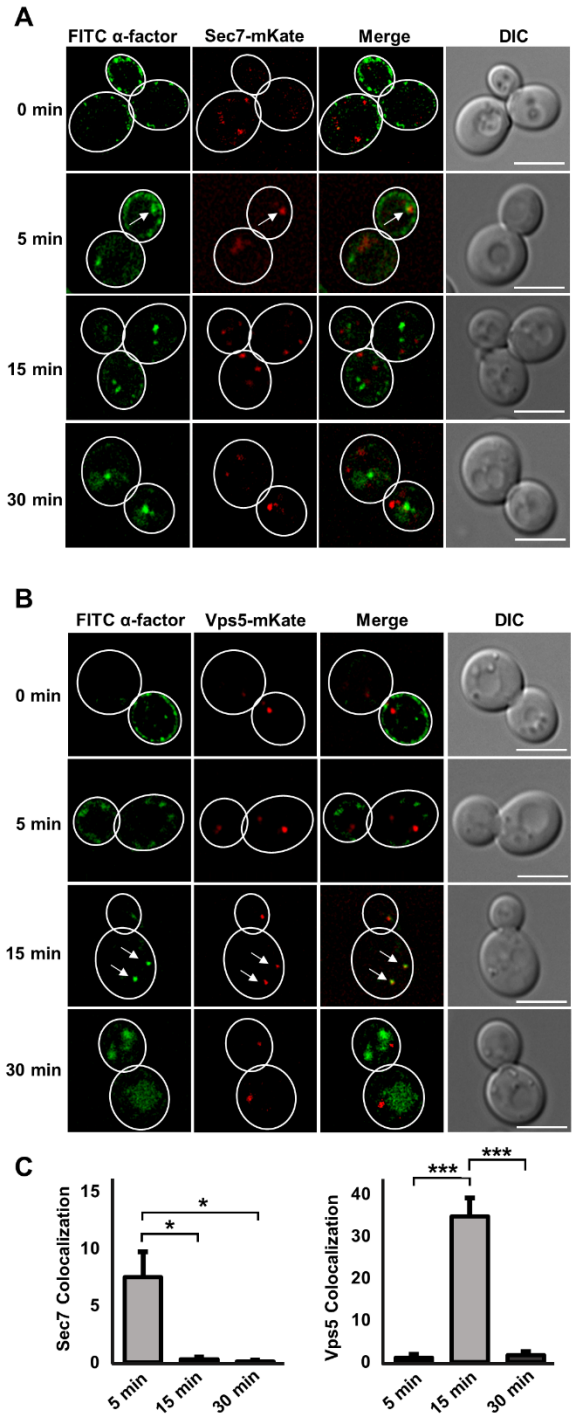

Figure 3. FITC α-factor is endocytosed at the PM and travels through the Golgi before the PVE. **(A)** Yeast Golgi marker Sec7-mKate was incubated with FITC α-factor and percent colocalization was calculated at time-points 0 min, 5 min, 15 min, and 30 min post-incubation. By 5 min ~100 percent of internalized α-factor was found in the Golgi (**C**, left graph) **(B)** Yeast PVE marker Vps5-mKate was incubated with FITC α-factor and percent colocalization was calculated at time-points 0 min, 5 min, 15 min, and 30 min

post-incubation. By 15 min ~100 percent of internalized α-factor was found in PVEs (**C**, right graph). Representative images of each time-point are shown. Arrows indicate colocalization between FITC α-factor and organelle markers. Statistical analysis was done using a single-factor ANOVA and Tukey's HSD test. * indicates $p < 0.05$, *** indicates $p < 0.001$. Scale bar indicates 5 μm.

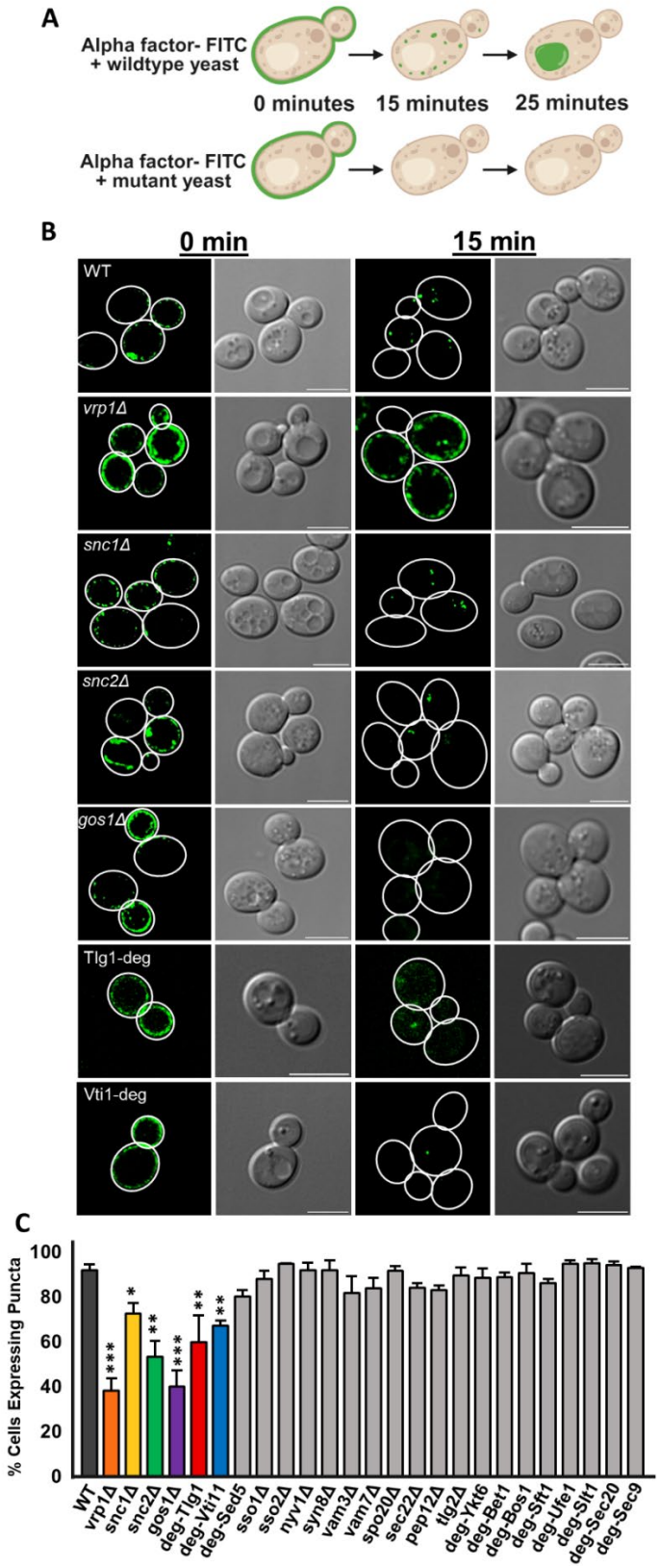

Figure 4. FITC α-factor uptake screen identifies Snc1, Snc2, Gos1, Tlg1, and Vti1 as PM-Golgi vesicle fusion machinery. **(A)** As described in Figure 3, FITC α-factor can be used

to visualize endocytic compartment in yeast. In wildtype cells, PM FITC α-factor travels to internal structures puncta in 5-15 minutes and is trafficked to the vacuole in 25 minutes. In PM-Golgi mutants, we see a reduction in the number of internal fluorescent puncta, providing a quantitative measurement of protein function in PM-TGN fusion. **(B)** Micrographs of internalized FITC α-factor in wildtype and indicated mutants. Clear defects are found in in *snc1Δ, snc2Δ*, *gos1Δ*, *tlg1Δ* and *vti1Δ* cells. **(C)** In total, twenty-four SNARE mutants were screened for loss of FITC α-factor internalization as compared to wildtype cells. ~95% of wildtype cells exhibited fluorescent puncta following 15 minutes of incubation at room temperature. A significant reduction of fluorescent puncta was found in *snc1Δ, snc2Δ, gos1Δ, tlg1Δ* and *vti1Δ* mutants. Note, vrp1Δ, a CME mutant was used as a negative control and indicates the amount of clathrin-independent endocytosis occurring. Statistical analysis was done using single-factor ANOVA and Tukey HSD test. * indicates $p < 0.05$, ** indicates $p < 0.01$, and *** indicates $p < 0.001$. Scale bar indicates 5 μm.

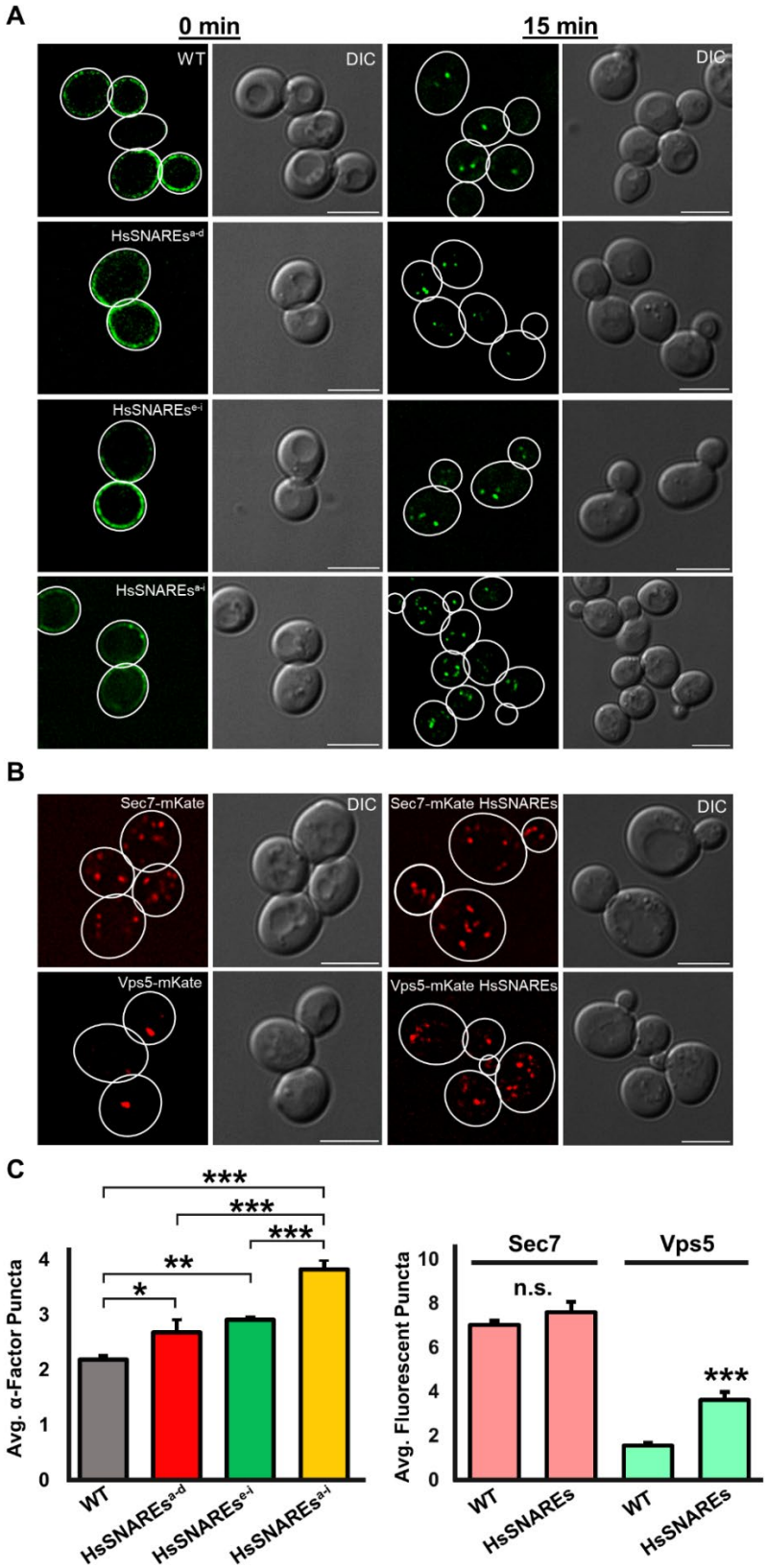

Figure 5. Heterologous expression of human SNAREs increases endosome complexity. **(A)** Humans have evolutionarily expanded their Golgi and endosomal SNARE proteins

as described in figure 1. Stx7[a], Stx8[b], Stx12[c], Vamp4[d], Stx6[e], Vamp7[f], Vamp8[g], Vti1A[h], and Vti1B[i] were heterologously expressed in yeast and screened for FITC α-factor uptake after 15 minutes. Combinational expression of Stx7[a], Stx8[b], Stx12[c], Vamp4[d] or Stx6[e], Vamp7[f], Vamp8[g], Vti1A[h], Vti1B[i] resulted in a 1.5-fold increase in internal fluorescent compartments. While simultaneous expression of all 9 SNARE proteins resulted in a 2-fold increase in internal fluorescent compartments (**C**, left graph). **(B)** The number of Golgi (Sec7-mKate) and PVE (Vps5-mKate) compartments were also visualized when all 9 human SNARE proteins were simultaneously expressed. The number of Golgi compartments did not change, however PVEs increased nearly 4-fold (**C**, right graph). Statistical analysis was done by single-factor ANOVA and Tukey's HSD test or Student's T-Test. * indicates $p < 0.05$, ** indicates $p < 0.01$, and *** indicates $p < 0.001$. Results represent the average of three experiments. Scale bar indicates 5 μm.

2.8 References

1. Elkin, S.R., A.M. Lakoduk, and S.L. Schmid, Endocytic pathways and endosomal trafficking: a primer. Wien Med Wochenschr, 2016. 166(7-8): p. 196-204.
2. Hong, W., SNAREs and traffic. Biochim Biophys Acta, 2005. 1744(2): p. 120-44.
3. Wang, T., L. Li, and W. Hong, SNARE proteins in membrane trafficking. Traffic, 2017. 18(12): p. 767-775.
4. Verhage, M. and J.B. Sorensen, Vesicle docking in regulated exocytosis. Traffic, 2008. 9(9): p. 1414-24.
5. Grosshans, B.L., D. Ortiz, and P. Novick, Rabs and their effectors: achieving specificity in membrane traffic. Proc Natl Acad Sci U S A, 2006. 103(32): p. 11821-7.
6. Prescianotto-Baschong, C. and H. Riezman, Morphology of the yeast endocytic pathway. Mol Biol Cell, 1998. 9(1): p. 173-89.
7. Day, K.J., J.C. Casler, and B.S. Glick, Budding Yeast Has a Minimal Endomembrane System. Dev Cell, 2018. 44(1): p. 56-72 e4.
8. Laidlaw, K.M.E., G. Calder, and C. MacDonald, Recycling of cell surface membrane proteins from yeast endosomes is regulated by ubiquitinated Ist1. J Cell Biol, 2022. 221(11).
9. Grissom, J.H., V.A. Segarra, and R.J. Chi, New Perspectives on SNARE Function in the Yeast Minimal Endomembrane System. Genes (Basel), 2020. 11(8).
10. Sollner, T., et al., A protein assembly-disassembly pathway in vitro that may correspond to sequential steps of synaptic vesicle docking, activation, and fusion. Cell, 1993. 75(3): p. 409-18.
11. Hong, W., SNAREs and traffic. Biochimica et Biophysica Acta, 2005. 1744: p. 120-144.
12. Yoon, T.Y. and M. Munson, SNARE complex assembly and disassembly. Curr Biol, 2018. 28(8): p. R397-R401.
13. Fabienne Paumet, V.R., James E. Rothman, The specificity of SNARE-dependent fusion is encoded in the SNARE motif. PNAS, 2004. 101: p. 3376-3380.
14. Weber, T., et al., SNAREpins: minimal machinery for membrane fusion. Cell, 1998. 92(6): p. 759-72.
15. Kienle, N., T.H. Kloepper, and D. Fasshauer, Phylogeny of the SNARE vesicle fusion machinery yields insights into the conservation of the secretory pathway in fungi. BMC Evol Biol, 2009. 9: p. 19.
16. Fasshauer, D., Structural insights into the SNARE mechanism. Biochim Biophys Acta, 2003. 1641(2-3): p. 87-97.
17. Tobias M. Hohl, F.P., Chritian Wimmer, James E. Rothman, Thomas H. Sollner, Harald Engelhardt, Arrangement of subunits in 20s particles consiting og NSF, SNAPs, and SNARE complexes. Molecular Cell, 1998. 2(5): p. 539-548.
18. Burri, L. and T. Lithgow, A complete set of SNAREs in yeast. Traffic, 2004. 5(1): p. 45-52.
19. Kloepper, T.H., C.N. Kienle, and D. Fasshauer, SNAREing the basis of multicellularity: consequences of protein family expansion during evolution. Mol Biol Evol, 2008. 25(9): p. 2055-68.

20. Edgar, R.C., MUSCLE: multiple sequence alignment with high accuracy and high throughput. Nucleic Acids Res, 2004. 32(5): p. 1792-7.
21. Stamatakis, A., RAxML version 8: a tool for phylogenetic analysis and post-analysis of large phylogenies. Bioinformatics, 2014. 30(9): p. 1312-3.
22. Darriba, D., et al., ProtTest 3: fast selection of best-fit models of protein evolution. Bioinformatics, 2011. 27(8): p. 1164-5.
23. Gietz, R.D., et al., Studies on the transformation of intact yeast cells by the LiAc/SS-DNA/PEG procedure. Yeast, 1995. 11(4): p. 355-60.
24. Guide to yeast genetics and molecular biology. Methods Enzymol, 1991. 194: p. 1-863.
25. Longtine, M.S., et al., Additional modules for versatile and economical PCR-based gene deletion and modification in Saccharomyces cerevisiae. Yeast, 1998. 14(10): p. 953-61.
26. Nishimura, K., et al., An auxin-based degron system for the rapid depletion of proteins in nonplant cells. Nat Methods, 2009. 6(12): p. 917-22.
27. Giuraniuc, C.V., M. MacPherson, and Y. Saka, Gateway vectors for efficient artificial gene assembly in vitro and expression in yeast Saccharomyces cerevisiae. PLoS One, 2013. 8(5): p. e64419.
28. Lee, M.E., et al., A Highly Characterized Yeast Toolkit for Modular, Multipart Assembly. ACS Synth Biol, 2015. 4(9): p. 975-86.
29. King, N., The unicellular ancestry of animal development. Dev Cell, 2004. 7(3): p. 313-25.
30. Brooke, N.M. and P.W. Holland, The evolution of multicellularity and early animal genomes. Curr Opin Genet Dev, 2003. 13(6): p. 599-603.
31. Blumer, K.J., J.E. Reneke, and J. Thorner, The STE2 gene product is the ligand-binding component of the alpha-factor receptor of Saccharomyces cerevisiae. J Biol Chem, 1988. 263(22): p. 10836-42.
32. Toshima, J.Y., et al., Spatial dynamics of receptor-mediated endocytic trafficking in budding yeast revealed by using fluorescent alpha-factor derivatives. Proc Natl Acad Sci U S A, 2006. 103(15): p. 5793-8.
33. McNew, J.A., et al., Gos1p, a Saccharomyces cerevisiae SNARE protein involved in Golgi transport. FEBS Lett, 1998. 435(1): p. 89-95.
34. Ma, M. and C.G. Burd, Retrograde trafficking and quality control of yeast synaptobrevin, Snc1, are conferred by its transmembrane domain. Mol Biol Cell, 2019. 30(14): p. 1729-1742.
35. Gerst, J.E., Conserved alpha-helical segments on yeast homologs of the synaptobrevin/VAMP family of v-SNAREs mediate exocytic function. J Biol Chem, 1997. 272(26): p. 16591-8.
36. Joost C.M. Holthius, B.J.N., Sadhana Dhruvakumar, Hugh R.B. Pelham, Two syntaxin homologues in the TGN/endosomal system of yeast. EMBO Journal, 1998. 17: p. 113-126.
37. John G. S. Coe, A.C.B.L., Jing Xu, Wanjin Hong, A Role for Tlg1p in the Transport of Proteins within the Golgi Apparatus of Saccharomyces cerevisiae. Molecular Biology of the Cell, 1999. 10: p. 2407–2423.
38. Gabriele Fischer von Mollard, S.F.N., Tom H. Stevens, The Yeast v-SNARE Vti1p Mediates Two Vesicle Transport Pathways through Interactions with the t-

SNAREs Sed5p and Pep12p. The Journal of Cell Biology, 1997. 137: p. 1511–1524.
39. Donnelly, S.F., et al., A proline-rich protein, verprolin, involved in cytoskeletal organization and cellular growth in the yeast Saccharomyces cerevisiae. Mol Microbiol, 1993. 10(3): p. 585-96.
40. Munn, A.L., et al., end5, end6, and end7: mutations that cause actin delocalization and block the internalization step of endocytosis in Saccharomyces cerevisiae. Mol Biol Cell, 1995. 6(12): p. 1721-42.
41. Sun, Y., A.C. Martin, and D.G. Drubin, Endocytic internalization in budding yeast requires coordinated actin nucleation and myosin motor activity. Dev Cell, 2006. 11(1): p. 33-46.
42. Heinrich, R. and T.A. Rapoport, Generation of nonidentical compartments in vesicular transport systems. J Cell Biol, 2005. 168(2): p. 271-80.
43. Fischer von Mollard, G. and T.H. Stevens, A human homolog can functionally replace the yeast vesicle-associated SNARE Vti1p in two vesicle transport pathways. J Biol Chem, 1998. 273(5): p. 2624-30.
44. Simonsen, A., et al., The Rab5 effector EEA1 interacts directly with syntaxin-6. J Biol Chem, 1999. 274(41): p. 28857-60.
45. Prekeris, R., et al., Differential roles of syntaxin 7 and syntaxin 8 in endosomal trafficking. Mol Biol Cell, 1999. 10(11): p. 3891-908.
46. He, Y. and M.E. Linder, Differential palmitoylation of the endosomal SNAREs syntaxin 7 and syntaxin 8. J Lipid Res, 2009. 50(3): p. 398-404.
47. Gaudet, P., et al., Phylogenetic-based propagation of functional annotations within the Gene Ontology consortium. Brief Bioinform, 2011. 12(5): p. 449-62.
48. Nishimoto-Morita, K., et al., Differential effects of depletion of ARL1 and ARFRP1 on membrane trafficking between the trans-Golgi network and endosomes. J Biol Chem, 2009. 284(16): p. 10583-92.
49. Miller, S.E., et al., A SNARE-adaptor interaction is a new mode of cargo recognition in clathrin-coated vesicles. Nature, 2007. 450(7169): p. 570-4.
50. Bilan, F., et al., Endosomal SNARE proteins regulate CFTR activity and trafficking in epithelial cells. Exp Cell Res, 2008. 314(11-12): p. 2199-211.
51. Advani, R.J., et al., Seven novel mammalian SNARE proteins localize to distinct membrane compartments. J Biol Chem, 1998. 273(17): p. 10317-24.
52. Shitara, A., et al., VAMP4 is required to maintain the ribbon structure of the Golgi apparatus. Mol Cell Biochem, 2013. 380(1-2): p. 11-21.
53. Burgo, A., et al., Role of Varp, a Rab21 exchange factor and TI-VAMP/VAMP7 partner, in neurite growth. EMBO Rep, 2009. 10(10): p. 1117-24.
54. Ward, D.M., et al., Syntaxin 7 and VAMP-7 are soluble N-ethylmaleimide-sensitive factor attachment protein receptors required for late endosome-lysosome and homotypic lysosome fusion in alveolar macrophages. Mol Biol Cell, 2000. 11(7): p. 2327-33.
55. Wong, S.H., et al., Endobrevin, a novel synaptobrevin/VAMP-like protein preferentially associated with the early endosome. Mol Biol Cell, 1998. 9(6): p. 1549-63.
56. Grote, E. and P.J. Novick, Promiscuity in Rab-SNARE interactions. Mol Biol Cell, 1999. 10(12): p. 4149-61.

57. Bethune, J. and F.T. Wieland, Assembly of COPI and COPII Vesicular Coat Proteins on Membranes. Annu Rev Biophys, 2018. 47: p. 63-83.
58. Cai, H., K. Reinisch, and S. Ferro-Novick, Coats, tethers, Rabs, and SNAREs work together to mediate the intracellular destination of a transport vesicle. Dev Cell, 2007. 12(5): p. 671-82.
59. Mossessova, E., L.C. Bickford, and J. Goldberg, SNARE selectivity of the COPII coat. Cell, 2003. 114(4): p. 483-95.
60. Yanguas, F. and M.H. Valdivieso, Analysis of the SNARE Stx8 recycling reveals that the retromer-sorting motif has undergone evolutionary divergence. PLoS Genet, 2021. 17(3): p. e1009463.
61. Tsui, M.M. and D.K. Banfield, Yeast Golgi SNARE interactions are promiscuous. J Cell Sci, 2000. 113 (Pt 1): p. 145-52.
62. Furukawa, N. and J. Mima, Multiple and distinct strategies of yeast SNAREs to confer the specificity of membrane fusion. Sci Rep, 2014. 4: p. 4277.

CHAPTER 4: CONCLUSION

In this dissertation, we have found that the SNARE proteins Snc1, Snc2, Gos1, Vti1, and Tlg1 mediate the fusion of PM-derived vesicles to the TGN in *Saccharomyces cerevisiae* using a combination of molecular phylogenetics and a novel endocytic assay that uses the yeast mating pheromone α-factor to visualize endocytosis (Figure 1A). Our findings support the yeast minimal endomembrane model proposed by Day et al in which the TGN acts as the primary acceptor of endocytic vesicles. Our phylogenetic analysis suggests that the homologs of yeast PVE associated SNAREs expanded multiple times across metazoan evolution. Expression of these endomembrane-associated SNAREs in budding yeast caused a marked increase in the amount of PVE compartments, visualized both with fluorescent α-factor assays and a PVE marker Vps5 (Figure 1B). In contrast, expression of these SNAREs did not produce a significant change in the number of TGN compartments within the cell. Collectively, these findings suggest that the expansion of endosome-associated SNAREs over the course of metazoan evolution played a significant role in the development of the complex endomembrane system that is observed in mammalian cells (Figure 1C).

Future directions will be aimed at conducting similar endocytic screens in other model eukaryotic species; namely, early branching metazoans. Previous analyses have shown two major SNARE expansions- first at the transition to multicellularity, and again at the rise of vertebrates. While endocytosis has been heavily studied in both yeast and vertebrate models, research involving the endomembrane of early-branching metazoan species is largely underrepresented. The investigation of these phyla is integral to

understanding the evolution of the metazoan endomembrane, as they represent an "intermediate" stage of endosomal SNARE expansion. We suspect that the general layout of the early-branching metazoan endomembrane will exhibit a hybrid of the minimal system observed in yeast and the complex system seen in vertebrates, perhaps with basic early endosomal structures that act as the primary endocytic accepting organelle- however significant molecular and phylogenetic analyses will need to be conducted to support these speculations.

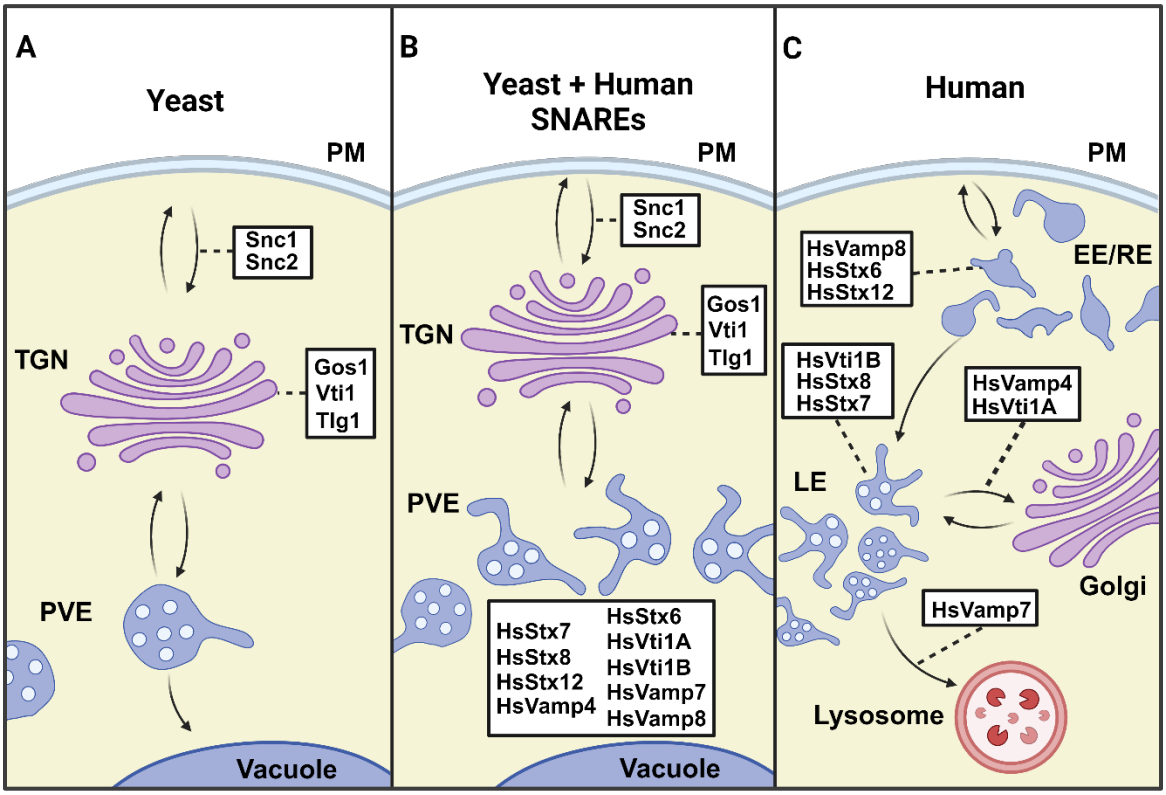

Figure 1. SNARE protein evolution and expansion drives endosome complexity model. **(A)** The yeast SNAREs Snc1, Snc2, Gos1, Vti1, and Tlg1 mediate PM-TGN vesicle fusion machinery. **(B)** Heterologous expression of human SNARE proteins Stx6, Stx7, Stx8, Stx12, Vti1A, VtiB, Vamp4, Vamp7, and Vamp8 increase number of endosomal compartments in yeast. **(C)** The expansion of endosomal SNARE proteins across metazoan evolution has significantly contributed to the development of a complex endomembrane system.

REFERENCES

1. Elkin, S.R., A.M. Lakoduk, and S.L. Schmid, *Endocytic pathways and endosomal trafficking: a primer.* Wien Med Wochenschr, 2016. **166**(7-8): p. 196-204.
2. Prescianotto-Baschong, C. and H. Riezman, *Morphology of the yeast endocytic pathway.* Mol Biol Cell, 1998. **9**(1): p. 173-89.
3. Kaksonen, M. and A. Roux, *Mechanisms of clathrin-mediated endocytosis.* Nat Rev Mol Cell Biol, 2018. **19**(5): p. 313-326.
4. Mettlen, M., et al., *Regulation of Clathrin-Mediated Endocytosis.* Annu Rev Biochem, 2018. **87**: p. 871-896.
5. Botstein, D., S.A. Chervitz, and J.M. Cherry, *Yeast as a model organism.* Science, 1997. **277**(5330): p. 1259-60.
6. Shaw, J.D., et al., *Yeast as a model system for studying endocytosis.* Exp Cell Res, 2001. **271**(1): p. 1-9.
7. Baggett, J.J. and B. Wendland, *Clathrin function in yeast endocytosis.* Traffic, 2001. **2**(5): p. 297-302.
8. Maria Antonietta De Matteis, A.L., *Exiting the Golgi complex.* Nature Reviews Molecular Cell Biology, 2008. **9**: p. 273-284.
9. Sollner, T., et al., *A protein assembly-disassembly pathway in vitro that may correspond to sequential steps of synaptic vesicle docking, activation, and fusion.* Cell, 1993. **75**(3): p. 409-18.
10. Burri, L. and T. Lithgow, *A Complete Set of SNAREs in Yeast.* Traffic, 2004. **5**(1): p. 45-52.
11. Hong, W., *SNAREs and traffic.* Biochimica et Biophysica Acta, 2005. **1744**: p. 120-144.
12. Wang, T., L. Li, and W. Hong, *SNARE proteins in membrane trafficking.* Traffic, 2017. **18**(12): p. 767-775.
13. Giaever, G. and C. Nislow, *The yeast deletion collection: a decade of functional genomics.* Genetics, 2014. **197**(2): p. 451-65.